ORIGINAL PAPER

Short-term fluctuations in vegetation and phytoplankton during the Middle Eocene greenhouse climate: a 640-kyr record from the Messel oil shale (Germany)

Olaf K. Lenz · Volker Wilde · Walter Riegel

Abstract The Palaeogene was the most recent greenhouse period on Earth. Especially for the Late Palaeocene and Early Eocene, several superimposed short-term hyperthermal events have been described, including extremes such as the Palaeocene–Eocene Thermal Maximum. Major faunal and floral turnovers in the marine and terrestrial realms were recorded in association with these events. High-resolution palynological analysis of the early Middle Eocene maar lake sediments at Messel, near Darmstadt, Germany, provides an insight into the dynamics of a climax vegetation during the Middle Eocene greenhouse climate in a time span without significant climatic excursions. Numerical techniques like detrended correspondence analysis and wavelet analysis have been applied to recognize cyclic fluctuations and long-term trends in the vegetation through a time interval of approximately 640 kyr. Based on the numerical zoning of the pollen diagram, three phases in the development of the vegetation may be distinguished. Throughout these phases, the climax vegetation did not change substantially in qualitative composition, but a trend towards noticeably less humid conditions probably in combination with a drop of the water level in the lake may be recognized. A shift in algal population from the freshwater dinoflagellate cyst *Messelodinium thielepfeifferae* to a dominance of *Botryococcus* in the uppermost part of the core is interpreted as a response to changes in acidity and nutrient availability within the lake. Time series analyses of pollen assemblages show that variations in the Milankovitch range of eccentricity, obliquity and precession can be distinguished. In addition, fluctuations in the sub-Milankovitch range are indicated. This demonstrates that floral changes during steady depositional conditions in the Middle Eocene of Messel were controlled by orbital forcing.

Keywords Middle Eocene · Maar lake · Palynology · Climate variability · Milankovitch cycles · Multivariate statistics · Time series analysis

O. K. Lenz (✉)
Institut für Angewandte Geowissenschaften,
Angewandte Sedimentgeologie, TU Darmstadt,
Schnittspahnstrasse 9, 64287 Darmstadt, Germany
e-mail: lenz@geo.tu-darmstadt.de

V. Wilde · W. Riegel
Senckenberg Forschungsinstitut und Naturmuseum,
Sektion Paläobotanik, Senckenberganlage 25,
60325 Frankfurt am Main, Germany
e-mail: volker.wilde@senckenberg.de

W. Riegel
e-mail: wriegel@gwdg.de

W. Riegel
Geowissenschaftliches Zentrum der Universität Göttingen,
Geobiologie, Goldschmidtstrasse 3, 37077 Göttingen, Germany

Introduction

The Palaeogene was a time of a warm "greenhouse" climate which climaxed in the Early Eocene when subtropical forests of the northern hemisphere spread beyond 60° N latitude (Harrington 2001). After the Early Eocene Climate Optimum (Zachos et al. 2001), a gradual cooling followed which led to the first continental-scale glaciations of Antarctica in the earliest Oligocene (Barrett 1996). Superimposed on the general climatic trend are several transient short-time hyperthermal events. Most prominent among them is the Palaeocene/Eocene Thermal Maximum (PETM

or ETM-1), an episode of ∼200 kyr of extreme global warming (e.g. Kennett and Stott 1991; Bains et al. 2000; Röhl et al. 2000), followed by other short-term events during the Early Eocene, such as the Elmo or ETM-2 (Lourens et al. 2005; Sluijs et al. 2009) and the "X" event (Röhl et al. 2005).

Numerous climate-related palaeobotanical studies on the Palaeocene and the Eocene focused on these so-called hyperthermal events, particularly on the question whether an important floral turnover was associated with the PETM in mid-latitudes of Europe (Beerling and Jolley 1998; Collinson et al. 2003) and North America (Wing et al. 2005, Harrington et al. 2004, Harrington et al. 2005, Harrington and Jaramillo 2007). However, their conclusions appear to be somewhat inconsistent and generally range from significant to moderate vegetation responses depending on the palaeogeographic position of the studied sections. Since the effects of Eocene hyperthermal events on vegetation appear not to be as dramatic as may be expected from a temperature increase of several degrees and a duration of about 200 kyr, it appears interesting to see whether any vegetation responses to ordinary Milankovitch cycles can be detected during stable greenhouse phases.

Here, we present a temporally highly resolved pollen record from the oil shale of the maar lake of Messel, Germany, spanning a period of 640 kyr within the early Middle Eocene, an episode of the Palaeogene greenhouse phase which was obviously not affected by hyperthermal events. The palynological study thus provides insights into the dynamics of a climax vegetation and serves as a record for vegetation changes and their potential cyclicity within the Palaeogene greenhouse system. Since annually laminated sediments of Quaternary maar lakes have been widely used as ideal archives of vegetation response to rapid climate change in an icehouse system (e.g. Stebich et al. 2009), the Messel oil shale may provide an important reference for understanding the effects of an equable warm climate and orbital forcing on vegetation.

Since the research well Messel 2001 was drilled in the centre of the former lake where a maximum thickness of the remaining lake sediments could be expected, a complete reference section of the Lower and Middle Messel Formation was obtained (Schulz et al. 2002) including 140 m of oil shale and 90 m of clastic lake sediments. This provided the opportunity for a high-resolution quantitative analysis of the palynological assemblages and corresponding time series analyses. The study aims at the recognition of any cyclic fluctuations and long-term trends throughout a time interval of 640 kyr during the Middle Eocene greenhouse climate. The oil shale of Messel is most suitable for that purpose since facies conditions and sedimentation rate remained stable for at least 640 kyr, and

changes in the vegetation therefore should have been exclusively caused by climate change. Thus, the deposits of the maar lake of Messel must be regarded as a unique and globally significant archive for the Middle Eocene climate system.

Linkage of the Palaeogene climate to orbital forcing has been proven by several recent studies (e.g. Röhl et al. 2000, 2003, 2004; Westerhold et al. 2007, 2008). Orbital forcing has been recorded for the Eocene from marine (e.g. Pälike et al. 2001; Lourens et al. 2005) and lacustrine sediments (e.g. Fischer 1986; Roehler 1993).

A pronounced reaction of the terrestrial flora to Milankovitch forcing has only been recorded starting from the latest Palaeogene thus far (Herrmann 2007), for instance from the Pliocene Pula maar in Hungary in the range of obliquity and precession (Willis et al. 1999) and of eccentricity and obliquity from the Miocene of Hungary and Spain (Jiménez-Moreno et al. 2005, 2007). Dinoflagellate and sporomorph records show precession driven climate variability in the high latitudes of the southeast Australian continent at the Antarctic margin in the Middle Eocene (Warnaar et al. 2009). However, little is known about the reaction of the terrestrial vegetation to the ordinary Milankovitch rhythms during the Palaeogene greenhouse mode in the (para)tropics. Some kind of climate cyclicity based on palynological data has been proposed for the Eocene by Krutzsch (1992), but this is not based on any statistical analyses.

Palaeogene maar lakes from central Germany that have been studied palynologically with high resolution are the Late Oligocene lake of Enspel and the Middle Eocene lake of Eckfeld. In contrast to the maar lake of Eckfeld where only general statements on climate change have been presented (Nickel 1996), the Enspel palynoflora shows cyclic fluctuations in the vegetation in the range of precession and obliquity (Herrmann 2007). In contrast to Messel, the age of the lake deposits of Enspel is younger (∼24.7 Ma; Mertz et al. 2007) and far outside the range of the Palaeogene greenhouse phase.

Based on spectral analyses of gamma ray logs and magnetic susceptibility from a previous well in the Messel oil shale, El Bay et al. (2001) suggested climatic changes induced by orbital parameters like eccentricity (96 kyr), obliquity (40, 53 kyr) and precession (20 ka), however, still without reference to confidence levels.

Geological situation

The oil shale of Messel is the best known among a series of isolated Palaeogene deposits (Felder et al. 2001) on the Sprendlinger Horst, the northern extension of the Odenwald basement, which is flanking the Upper Rhine Graben

to the northeast in Southwest Germany (Fig. 1). These deposits represent individual volcanic and tectonic structures which are Middle Eocene in age and predate the later Rhine Graben system (e.g. Harms 2001; Jacoby et al. 2005). The Middle Eocene lake sediments of the Messel pit were defined as the "Messel Formation" which typically consists of highly bituminous shales. A continuous core ("Messel 2001") drilled in the centre of the basin recovered massive volcanoclastic deposits (diatreme breccia, lapilli tuffs) between 433 m and 228 m the discovery of which ultimately proved that the overlying lake sediments have been deposited within a maar structure (Lorenz 2000; Schulz et al. 2002). The maar diatreme was formed by a phreatomagmatic eruption (Lorenz 2000; Schulz et al. 2002; Harms et al. 2003; Felder and Harms 2004) very early during the magneto-chron C21r (47.9–49.0 Myr) (Mertz and Renne 2005; Rolf et al. 2005).

A generalized lithologic succession encountered in core Messel 2001 is shown in Fig. 2. The Lower Messel Formation above 228 m represents the Initial Lake Phase of Lenz et al. (2007a). The Middle Messel Formation above 94 m is almost identical with the classical "Messel Oil Shale", the finely laminated highly bituminous shale which was formed during a long-term stable meromictic phase of the lake (Fig. 3). This oil shale has been the target of intense mining operations between the 1870s and 1974 (Schaal and Schneider 1995), leaving the present "Messel pit". The Upper Messel Formation is only preserved in small remnants at the margin of the Messel pit and probably represents the gradual terrestrialization of the lake (Harms et al. 2003), but its relation to the Middle Messel Formation is not known in detail.

Above 94 m, the Messel oil shale is characterized by a very fine light and dark lamination. The time series analyses presented here are based on the assumption that this lamination reflects an annual varve-like stratification (Fig. 3). This was originally suggested for the Middle Messel Formation by Irion (1977) and supported by Goth (1990) who studied the distribution of palynomorphs in individual laminae by SEM. It follows, therefore, that the oil shale is essentially made up of couplets of spring/summer layers mainly composed of algae (*Tetraedron minimum*) and dark autumn/winter layers mainly composed of terrigenous background sediment. On this basis, Goth (1990) determined a sedimentation rate of 0.15 mm/year by counting oil shale laminae. El Bay et al. (2001) calculated a comparable sedimentation rate of 0.146 ± 0.052 mm/year for an older well by using gamma ray logs and magnetic susceptibility. Similar data from the new core Messel 2001 indicate a sedimentation rate of 0.14 mm/year (Schulz et al. 2002). We therefore accept annual stratification as the basis for the time scale in our analyses and assume continuous sedimentation at a constant rate throughout our study interval.

Following initial palynological studies of the Messel oil shale by Pflug (1952, 1957) and Thomson and Pflug (1953), Thiele-Pfeiffer (1988) published a thorough systematic and taxonomic palynological monograph of the oil shale, based on a previous core from Messel (core 4/1980: Weber and Hofmann 1982; Liebig 2001) which, however, did not penetrate into the oil shale free lake sediments at the base of the Messel Formation. An initial numerical analysis of Thiele-Pfeiffer's data by Lenz et al. (2005) showed that the composition of pollen assemblages is not as homogenous throughout the sequence as originally stated by Thiele-Pfeiffer (1988). For the initial phase of the

Fig. 1 Geological map showing the location of the Messel pit in relation to other Palaeogene sites in the area (modified after Harms et al. 1999)
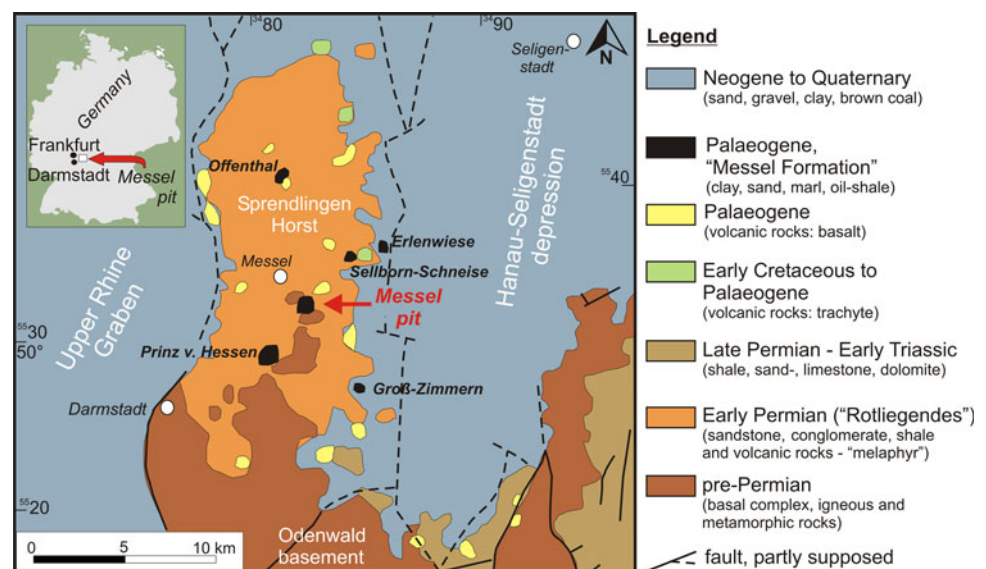
Fig. 2 **a** Generalized section of the Messel 2001 core (after Felder and Harms 2004). **b** The stratigraphic position of the Messel Formation: comparison of the Messel Formation related to the magnetostratigraphic (*GPTS* global polarity time scale) and biochronologic (*ELMA* European land mammal age) time scales (after Mertz and Renne 2005)
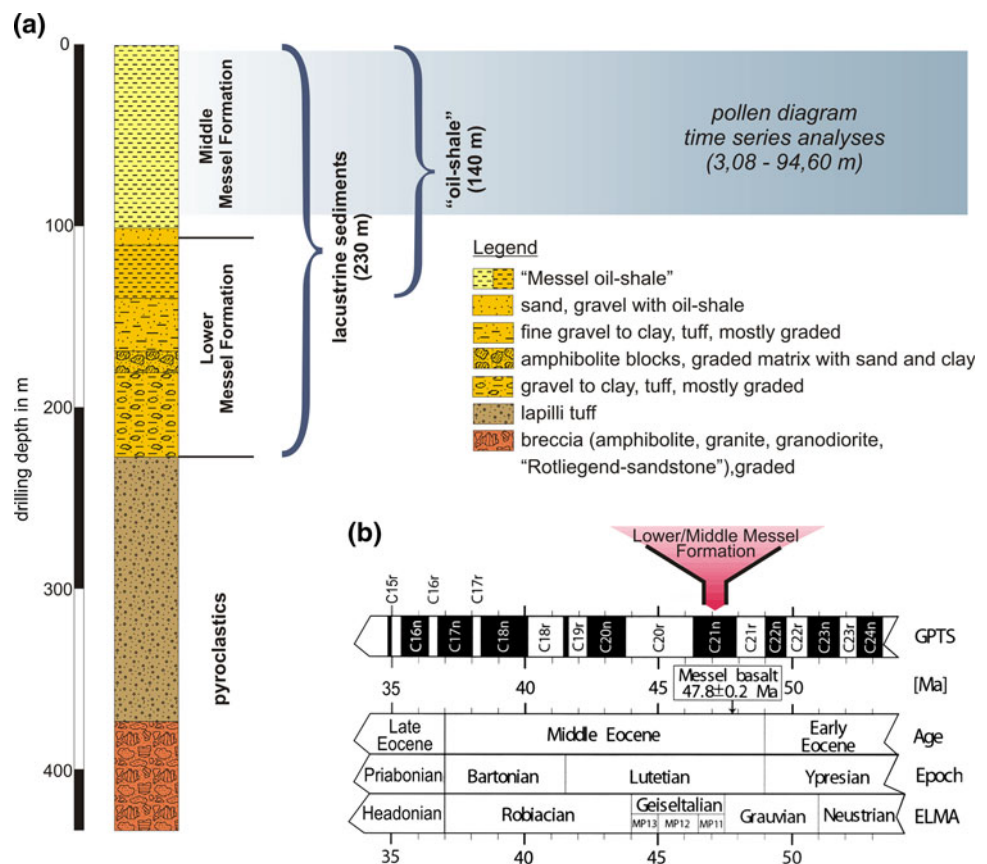
lake, we have been able to show how the climax vegetation gradually recolonized the crater wall and the surrounding area after the eruption (Lenz et al. 2007a).

Materials and methods

Sampling and sample processing

The present analysis is restricted to the Middle Messel Formation between 3.08 and 94.60 m of the core since this interval represents the homogeneously laminated oil shale indicating stable meromictic conditions in the lake (Fig. 2).

The laminated oil shale was sampled by removing 1-cm slices at 10-cm intervals. In our study, 458 samples were analysed palynologically by using an equal sample distance of 20 cm. All samples were treated with HCl, HF and KOH following the standard procedures described in Kaiser and Ashraf (1974). In addition, the residue was sieved with a mesh size of 10 μm. Some of the residues were slightly oxidized by applying diluted HNO_3 in order to remove flocculating organic matter and to improve transparency of individual palynomorphs.

Raw material, residues and slides of all samples are stored in the Senckenberg Forschungsinstitut und Naturmuseum, Frankfurt am Main, Germany.

Identification of palynomorphs

Identification of pollen and spores is primarily based on the systematic–taxonomic study of Thiele-Pfeiffer (1988). A minimum of 300 individual sporomorphs per sample were counted at 400 times magnification. Altogether, 97 different taxa of pollen and spores were identified in the Middle Messel Formation (Table 1). Identifiable remains of algae such as *Botryococcus* or cysts of dinoflagellates and Zygnemataceae (*Ovoidites*) were also counted. All 458 samples contained sufficient palynomorphs, but preservation of the individual specimens is only moderate throughout the oil shale. Thus, a relatively high proportion of 10–20% of the total assemblage could not be positively determined and was recorded as "Varia".

The pollen diagrams were produced by PanPlot 10.16 (Alfred Wegener Institut für Polare und Marine Forschung, PANGEA). Pollen and spores were calculated to 100%, while the values for algae are plotted as additional percentages (% of the total pollen sum). The taxa are arranged according to their weighted average value (WA regression, ter Braak and Looman 1995) in relation to depth by means of TRAN 1.81 (S. Juggins, University of Newcastle), because an arrangement of pollen curves is necessary to obtain ecologically useful groups (Janssen and Birks 1994).
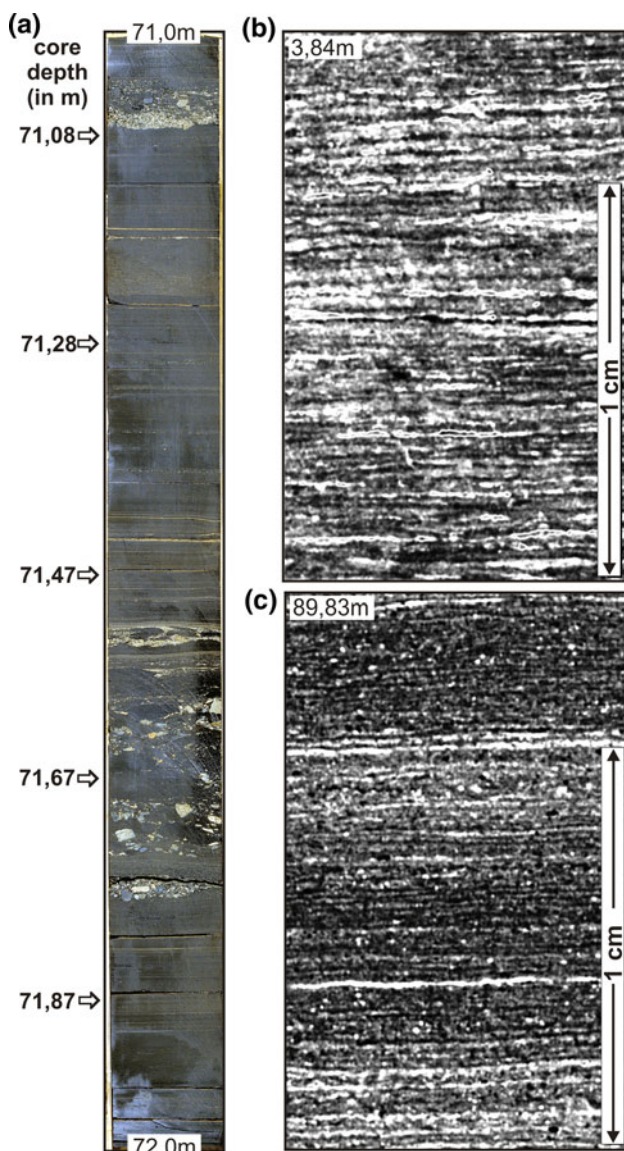
Fig. 3 a A selected lithologic section of the Messel 2001 core between 71 and 72 m, showing laminated oil shale and reworked sediments with extraclasts. *Arrows* indicate position of samples. Based on photographs of FIS/HLUG 2001: 12051.pcd–12053.pcd. **b, c** High-resolution core micrographs from 3.84 and 89.83 m core depth, showing an annual stratification represented by a light spring/summer algal layer (*Tetraedron minimum* layer) and a dark autumn/winter layer composed of terrigenous background sediment

Statistical evaluation

Because of the great diversity including more than 97 species of pollen and spores and the limited quality of preservation, the number of variables, i.e. families, genera or individual species, has been limited to 52 (Table 1) for numerical analyses. Thereby, taxa were excluded from statistical analysis, which are very rare (average frequency < 1.5%). Other taxa such as various species of *Plicatopollis* were lumped in order to minimize errors in

identification of individual "species". By applying this approach, loss of information is expected to be minimal.

The program PSIMPOLL 4.10 (Bennett 2005) was used for numerical zoning, randomization tests and zoning modelling. Because of the dominance of few palynomorphs, the frequency data were normalized by square-root transformation. In this way, rare taxa are upweighted to abundant ones (Kovach 1989). This is especially important since the pollen spectra are dominated by only few elements (*Plicatopollis plicatus*, *Tricolpopollenites liblarensis* and *Tricolporopollenites cingulum*) that suppress the other elements in the percentage rate by their mass occurrence.

For numerical treatment of the palynological data, Detrended Correspondence Analyses (Hill and Gauch 1980) were implemented using the software PAST 1.67 (Hammer et al. 2001). For this purpose, percentage values of individual species were grouped into frequency classes. Frequency classes minimize the effect of minor fluctuations in percentage values, but, at the same time, preserve and emphasize the most important signals. Following Gauch (1982), nine cut levels (0 to <0.5 to <1 to <2 to <4 to <8 to <16 to <32 to <64%) were defined for the sporomorph percentages.

For time series analysis, the number of variables has been further reduced by excluding the algae (*Botryococcus*, dinocysts and *Ovoidites*). The remaining statistically significant palynomorphs were subsequently grouped into 8 groups according to their frequency distribution by means of cluster analysis (Table 2, Fig. 8; Ward's method, software: PAST 1.67, Hammer et al. 2001). The resulting frequency graphs of Fig. 9 are the database for our time series analyses. The frequency distribution of the respective clusters turned out to be quite similar to the frequency distribution of individual taxa, but clustering has been applied to improve the statistical significance of the time series signals and to consider elements with low frequencies within the pollen spectrum.

To assess persistent patterns in pollen precipitation, we employed two independent techniques of spectral analysis. First, we applied the Morlet wavelets (Morlet 1983; Torrence and Compo 1998), a continuous wavelet transform, proven and tested in climate time series analysis (Lau and Weng 1995; Dunca et al. 2009; Schöne and Fiebig 2009; Wanamaker et al. 2009). The transform was based on the method described in Torrence and Compo (1998) by means of Wavelet software provided by these authors. Wavelet transforms have the advantage that they can be used to evaluate time series that are non-stationary and contain a variety of frequencies (Daubechies 1990). Since the individual taxa are distributed within the section with great fluctuations and do not always occur with significant values, our pollen data show a typical non-stationary signal.

Table 1 List of variables and palynomorphs used for pollen diagram, numerical and time series analyses

Leiotriletes spp.

  Leiotriletes maxoides Krutzsch 1962 (Schizaeaceae, *Lygodium*—climbing fern)

  Leiotriletes microadriennis Krutzsch 1959 (Schizaeaceae?—climbing fern)

  Leiotriletes kopeckii Kedves 1973 (Polypodiaceae, *Pteridium*; Cyatheaceae?)

Other Triletes

  Cicatricosisporites dorogensis R. Potonié & Gelletich 1933 (Parkeriaceae?, Schizaeaceae?, Polypodiaceae?)

  Cicatricosisporites paradorogensis Krutzsch 1959 (Schizaeaceae—climbing fern)

  Trilites menatensis Kedves 1982 (?)

  Trilites solidus (R. Potonié 1934) Krutzsch 1959 (Schizaeaceae, *Lygodium*—climbing fern)

  Trilites sp. (?)

  Concavisporites (Obtusisporis) minimus Krutzsch 1962 (?)

  Baculatisporites primarius (Wolf 1934) Thomson & Pflug 1953 (Osmundaceae, *Osmunda*)

  Ischyosporites tertiarius Krutzsch 1967 ex Roche 1973 (?)

  Retitriletes belgicus Krutzsch & Vanhoorne 1977 (?)

  Echinatisporis sp. (Selaginellaceae, *Selaginella*)

  Tegumentisporis sculpturoides (Krutzsch 1959) Krutzsch 1963 (Selaginellaceae, *Selaginella*)

  Tegumentisporis villosoides (Krutzsch 1959) Krutzsch 1963 (Selaginellaceae, *Selaginella*)

  Tegumentisporis tegumentis (Krutzsch 1959) Krutzsch 1963 (Selaginellaceae, *Selaginella*)

Polypodiaceae (trilete spores)

  Polypodiaceoisporites lusaticus Krutzsch 1967 (Polypodiaceae, *Pteris*)

  Polypodiaceoisporites gracillimus Nagy 1963 (Polypodiaceae, *Pteris*)

  Polypodiaceoisporites sp. (Polypodiaceae, *Pteris*)

  Verrucingulatisporites undulatus Nagy 1963 (Polypodiaceae, *Pteris*)

Laevigatosporites spp.

  Laevigatosporites haardtii (R. Potonié & Venitz 1934) Thomson & Pflug 1953 (Polypodiaceae)

  Laevigatosporites discordatus Pflug 1953 (Polypodiaceae)

Verrucatosporites spp.

  Verrucatosporites favus (R. Potonié 1931) Thomson & Pflug 1953 (Polypodiaceae, *Polypodium*)

  Verrucatosporites microfavus Thiele-Pfeiffer 1988 (Polypodiaceae)

  Verrucatosporites pseudoregulatius Krutzsch 1967 (Polypodiaceae)

  Verrucatosporites cellarius (Krutzsch 1959) Krutzsch 1967 (Polypodiaceae)

Pinaceae

  Pityosporites labdacus (R. Potonié 1931) Thomson & Pflug 1953 (Pinaceae, *Pinus*)

Table 1 continued

Cupressaceae/Taxodiaceae

  Inaperturopollenites concedipites (Wodehouse 1933) Krutzsch 1971 (Taxodiaceae, *Glyptostrobus*)

  Cupressacites insulipapillatus (Trevisan 1967) Krutzsch 1971 (Taxodiaceae, Cupressaceae)

Chloranthaceae

  Emmapollis pseudoemmaensis Krutzsch 1970 (Chloranthaceae, *Ascarinopsis*?, *Ascarina*?)

Nymphaeaceae

  Monocolpopollenites crassiexinus Thiele-Pfeiffer 1988 (Nymphaeaceae, *Nymphaea*?)

Palmae

  Monocolpollenites tranquillus (R. Potonié 1934) Thomson & Pflug 1953 (Palmae, *Phoenix*)

Hydrocharitaceae

  Punctilongisulcites microechinatus Thiele-Pfeiffer 1988 (Hydrocharitaceae)

P. pseudoexcelsus

  Plicapollis pseudoexcelsus (Krutzsch 1957) Krutzsch 1961 (Juglandaceae—Walnut Family)

  Plicapollis pseudoexcelsus (Krutzsch 1957) Krutzsch 1961 *microturgidus* Pflug 1953 (Juglandaceae—Walnut Family)

T. excelsus

  Triatriopollenites excelsus (R. Potonié 1931) Thomson & Pflug 1953 (Myricaceae, Juglandaceae?)

T. excelsus minor

  Triatriopollenites excelsus (R. Potonié 1931) Thomson & Pflug 1953 *minor* Pflug 1953 (Myricaceae, Juglandaceae?)

T. rurensis/bituitus

  Triatriopollenites rurensis Thomson & Pflug 1953 (Myricaceae, *Myrica*)

  Triatriopollenites bituitus (R. Potonié 1931) Thomson & Pflug 1953 (Myricaceae, *Myrica*)

Plicatopollis spp.

  Plicatopollis plicatus (R. Potonié 1934) Krutzsch 1962 (Juglandaceae—Walnut Family)

  Plicatopollis hungaricus Kedves 1974 (Juglandaceae—Walnut Family)

  Plicatopollis lunatus Kedves 1974 (Juglandaceae—Walnut Family)

  Labraferoidaepollenites menatensis Kedves 1982 (Juglandaceae—Walnut Family, *Engelhardia*?)

Momipites spp.

  Momipites punctatus (R. Potonié 1931) Nagy 1969 (Juglandaceae—Walnut Family, *Engelhardia*?, *Oreomunnea*?, *Alfaroa*?)

  Momipites quietus (R. Potonié 1931) Nichols 1973 (Juglandaceae—Walnut Family, *Engelhardia*)

Platycarya

  Platycaryapollenites platycaryoides (Roche 1969) Kedves 1982 (Juglandaceae—Walnut Family, *Platycarya*)

  Platycaryapollenites miocaenicus Nagy 1969 (Juglandaceae—Walnut Family, *Platycarya*)

  Platcacaryapollenites semicyclus (Krutzsch & Vanhoorne 1977) Thiele-Pfeiffer 1988 (Juglandaceae—Walnut Family, *Platycarya*)

Table 1 continued

Carya

  Caryapollenites triangulus (Pflug 1953) Krutzsch 1961
  (Juglandaceae—Walnut Family, *Carya*)

  Caryapollenites circulus (Pflug 1953) Krutzsch 1961
  (Juglandaceae—Walnut Family, *Carya*)

Pterocarya

  Pterocaryapollenites stellatus (R. Potonie 1931) Thiergart 1937
  (Juglandaceae—Walnut Family, *Pterocarya*)

Subtriporopollenites spp.

  Subtriporopollenites anulatus Thomson & Pflug 1953 *nanus*
  Thomson & Pflug 1953 (Juglandaceae—Walnut Family)

  Subtriporopollenites constans Pflug 1953 (?)

T. rhenanus/robustus

  Triporopollenites rhenanus (Thoms. in R. Pot., Thoms. & Thierg.
  1950) Th. & Pf. 1953 (Betulaceae—Birch Family, *Ostrya*)

  Triporopollenites robustus Pflug 1953 (?Betulaceae—Birch Family)

Ulmaceae

  Polyporopollenites eoulmoides Krutzsch & Vanhoorne 1977
  (Ulmaceae)

  Polyporopollenites undolosus (Wolf 1934) Thomson & Pflug
  1953 (Ulmaceae, *Ulmus, Zelkova*)

  Polyporopollenites verrucatus Thiele-Pfeiffer 1980 (Ulmaceae,
  Hemiptelea)

Celtis

  Celtipollenites intrastructurus (Krutzsch & Vanhoorne 1977)
  Thiele-Pfeiffer 1980 (Ulmaceae, *Celtis*)

  Celtipollenites laevigatus Thiele-Pfeiffer 1988 (Ulmaceae)

Tiliaceae/Bombacaceae

  Various species of the genus *Intratriporopollenites* Thomson &
  Pflug 1953 (Tiliaceae, Bombacaceae)

Symplocaceae

  Porocolpopollenites rarobaculatus Thiele-Pfeiffer 1980
  (Symplocaceae, *Symplocus*)

  Porocolpopollenites vestibulum (R. Potonié 1931) Thomson &
  Pflug 1953 (Symplocaceae, *Symplocus?*)

  Symplocospollenites orbis (Thomson & Pflug 1953) R. Potonié
  1960 (Symplocaceae, *Symplocos?*)

Labrapollis labraferus

  Labrapollis labraferus (R. Potonié 1931) Krutzsch 1968 (?)

Icacinaceae

  Compositoipollenites rhizophorus (R. Pot 1934) R. Pot. 1960 ssp.
  burghasungensis (Mürriger & Pflug 1952) Thomson &
  Pflug 1953 (Icacinaceae, *Polyporandra, Iodes?*)

  Compositoipollenites minimus Krutzsch & Vanhoorne 1977
  (Icacinaceae)

Pentapollenites spp.

  Pentapollenites pentangulus (Pflug 1953) Krutzsch 1957
  pentangulus Krutzsch 1962 (?)

  Pentapollenites pentangulus (Pflug 1953) Krutzsch 1957
  foveostriatus Krutzsch 1962 (?)

T. liblarensis/quisqualis

  Tricolpopollenites liblarensis (Thoms. in R. Pot., Thoms. &
  Thierg. 1950) Th. & Pf. 1953 *liblarensis* (Thoms. in R. Pot.,
  Thoms. & Thierg. 1950) Th. & Pf. 1953 (Fagaceae, Fabaceae,
  Combretaceae, Verbenaceae)

Table 1 continued

  Tricolpopollenites liblarensis (Thoms. in R. Pot., Thoms. &
  Thierg. 1950) Th. & Pf. 1953 *fallax* (R. Potonié 1934)
  Thomson & Pflug 1953 (Fagaceae, Fabaceae, Combretaceae,
  Verbenaceae)

  Tricolpopollenites quisqualis (R. Potonie 1934) Thomson &
  Pflug 1953 (Fagaceae?)

T. asper

  Tricolpopollenites asper Thomson & Pflug 1953
  (Fagaceae—Beech Family, *Quercus*)

T. retiformis

  Tricolpopollenites retiformis Thomson & Pflug 1953
  (Salicaceae, *Salix*)

T. vegetus

  Tricolpopollenites vegetus (R. Potonié 1934) Krutzsch 1959
  (Hamamelidaceae?)

T. cingulum

  Tricolporopollenites cingulum (R. Potonie 1931) Thomson &
  Pflug 1953 *fusus* (R. Potonie 1931) Thomson & Pflug 1953
  (Fagaceae, *Castanopsis?*)

  Tricolporopollenites cingulum (R. Potonie 1931) Thomson &
  Pflug 1953 *pusillus* (R. Potonie 1934) Thomson & Pflug 1953
  (Fagaceae, *Castanopsis, Lithocarpus, Pasania*)

  Tricolporopollenites cingulum (R. Potonie 1931) Thomson &
  Pflug 1953 *oviformis* (R. Potonie 1931) Thomson & Pflug
  1953 (Fagaceae, *Castanea, Castanopsis, Lithocarpus, Pasania*)

T. satzveyensis

  Tricolporopollenites satzveyensis Pflug 1953 (Mastixiaceae)

T. edmundii

  Tricolporopollenites edmundii (R. Potonié 1931) Thomson &
  Pflug 1953 (Mastixiaceae)

T. marcodurensis

  Tricolporopollenites marcodurensis Thomson & Pflug 1953
  (Vitaceae)

T. microreticulatus

  Tricolporopollenites microreticulatus Thomson & Pflug 1953
  (Oleaceae)

T. parmularius

  Tricolporopollenites parmularius (R. Potonié 1934) Kr. in Kr.,
  Pch. & Spieg. 1960 (Eucommiaceae, *Eucommia*)

T. microporitus

  Tricolporopollenites microporitus Thomson & Pflug 1953
  (Hamamelidaceae?, Verbenaceae?, Oleaceae?)

T. solé de portai

  Tricolporopollenites solé de portai Kedves 1965
  (Anacardiaceae, Rosaceae)

T. mansfeldensis

  Tricolporopollenites mansfeldensis Krutzsch 1969 (?)

T. quercioides

  Tricolporopollenites cf. *quercioides* Krutzsch & Vanhoorne
  1977 (?)

T. messelensis

  Tricolporopollenites messelensis Thiele-Pfeiffer 1988

T. abbreviatus

  Tricolporopollenites abbreviatus (R. Pot. 1934)
  Krutzsch 1961 (?)

Table 1 continued

Nyssapollenites spp.

  Nyssapollenites kruschii (R. Pot. 1931) Nagy 1969 *analepticus* (R. Pot. 1934) Nagy 1969 (Nyssaceae, *Nyssa*)

  Nyssapollenites kruschii (R. Pot. 1931) R. Pot., Th. & Thierg. 1950 *accessorius* (R. Pot. 1934) R. Pot., Th. & Thierg. 1950 ex Simoncsics 1969 (Nyssaceae, *Nyssa*)

Araliaceoipollenites spp.

  Araliaceoipollenites euphorii (R. Potonié 1931) R. Potonié 1951 (Araliaceae)

  Araliaceoipollenites reticuloides Thiele-Pfeiffer 1980 (Araliaceae, *Hedera*)

Tetracolporopollenites spp.

  Tetracolporopollenites sapotoides Thomson & Pflug 1953 (Sapotaceae)

  Tetracolporopollenites manifestus (R. Potonié 1931) Thomson & Pflug 1953 (Sapotaceae)

Ericaceae

  Ericipites callidus (R. Potonié 1931) Krutzsch 1970 (Ericaceae)

  Ericipites ericius (R. Potonié 1931) R. Potonié 1960 (Ericaceae)

Dinoflagellates

  Messelodinium thielepfeifferae Lenz, Wilde, Riegel & Heinrichs 2007

Botryococcus

  Botryococcus sp.

Ovoidites

  Ovoidites sp.

Detailed taxonomic information on the listed species: see Thomson and Pflug (1953), Krutzsch and Vanhoorne (1977), Thiele-Pfeiffer (1980, 1988), Krutzsch (2004) and Lenz (2005)

Wavelet analyses transform a time series into time–frequency space visualizing dominant modes of variability and their variation with time (Torrence and Compo 1998).

In addition, spectral analysis was carried out using the program REDFIT 3.8 to test whether peaks in the spectrum of a time series are significant against a red-noise background from a first-order autoregressive (AR1) process (Schulz and Mudelsee 2002).

Age model

Based on a constant sedimentation rate of 0.14 mm/yr, our sample distance of 20 cm corresponds to about 1,400 years. Transformation of the total sampled depth into a time scale (Fig. 9) results in an exceptionally long high-resolution continental record of 640 kyr represented by 91.6 m of oil shale in our core. Thus, except for long eccentricity with a period of 400 kyr the temporal scale of our study should resolve any cycles and trends within the range of the classical Milankovitch frequency band as reflected by the vegetation surrounding the Messel lake.

Results

Pollen zonation

In the pollen diagram for the Middle Messel Formation above the event bed (Fig. 4), taxa are arranged based on the weighted average regression with depth as the predictor variable (Janssen and Birks 1994; ter Braak and Looman 1995). The diagram shows that most of the elements occur over the entire Middle Messel Formation, and changes are restricted to frequency variations.

In order to detect any underlying trend of palaeoecological significance in the relatively uniform pollen spectra, the "optimal splitting by information content" (OSIC; Bennett 2005) is used here to establish a robust zonation. It should be noted that the remains of algae were included in the calculation of the zoning since their dominance within parts of the section is important for the delimitation of the individual zones. As a result, the following six zones are distinguished (Fig. 4).

Zone 1 (94.79–74.28 m)

Zone 1 includes 104 equidistant samples across 20.51 m and covers approximately 143 kyr. Most remarkable for this zone is the abundance of cysts of freshwater dinoflagellates. These cysts, which were noted for the first time in Messel by Thiele-Pfeiffer (1988) and described as *Messelodinium thielepfeifferae* by Lenz et al. (2007b), represent an important component of the primary production in the lake. This is reflected in values of up to 20% for *Messelodinium* in zone 1, while evidence of other algae like the coccal green alga *Botryococcus* is lacking.

Among the great number of pteridophyte spore taxa known from Messel (Thiele-Pfeiffer 1988), some show their peak abundance in the lower part of the Middle Messel Formation. This is especially true for smooth trilete spores of the genus *Leiotrilletes* which occur in high frequencies in zones 1 and 2. According to Thiele-Pfeiffer (1988), they are mostly attributable to Schizaeaceae and Polypodiaceae s.l., but generic affinities remain unclear. During the initial recolonization of the volcanic site, ferns formed important elements of a pioneering vegetation (Lenz et al. 2007a). Most probably, they later remained important elements of the vegetation along the shoreline and in marginal herbaceous swamps (Wilde 1989).

Similarly, the pollen of the aquatic Hydrocharitaceae, represented by *Punctilongisulcites microechinatus* (Thiele-Pfeiffer 1988), although not very frequent, reaches its maximum abundance in zones 1 and 2. Thiele-Pfeiffer (1988) found close similarities to pollen of the extant genera *Blyxa*, *Ottelia* and *Stratiotes*, which are entomophilous (Tanaka et al. 1997) and therefore poor pollen

Table 2 List of the eight clusters and their palynomorph content (see cluster analysis, Fig. 8)

Cluster no.	Palynomorph content
Cluster 1	*Platycarya*
	Plicapollis pseudoexcelsus
	Pinaceae
Cluster 2	Ulmaceae (*Ulmus/Zelkova*)
	Tricolporopollenites microreticulatus
	Tricolporopollenites parmularius
	Labrapollis labraferus
Cluster 3	*Triporopollenites rhenanus/robustus*
	Icacinaceae
	Polypodiaceae (trilete spores)
	Tricolporopollenites abbreviatus
	Tricolporopollenites edmundii
	Symplocaceae
	Other Triletes (without Selaginellaceae)
	Selaginellaceae
	Tricolporopollenites mansfeldensis
	Nymphaeaceae
	Hydrocharitaceae
	Tricolporopollenites quercioides
	Araliaceoipollenites spp.
	Palmae
	Ericaceae
	Tricolporopollenites messelensis
Cluster 4	*Tricolpopollenites retiformis*
	Tricolpopollenites vegetus
	Tricolporopollenites microporitus
	Nyssapollenites spp.
	Tiliaceae/Bombacaceae
	Tricolporopollenites satzveyensis
	Pentapollenites spp.
	Tricolporopollenites marcodurensis
	Triatriopollenites rurensis/bituitus
Cluster 5	*Tricolporopollenites solé de portai*
	Celtis
	Subtriporopollenites spp.
	Leiotriletes spp.
Cluster 6	*Pterocarya/Carya*
	Momipites spp.
	Tetracolporopollenites spp.
	Cupressaceae/Taxodiaceae
	Chloranthaceae
	Polypodiaceae (monolete spores)
	Laevigatosporites spp.
	Verrucatosporites spp.
	Triatriopollenites excelsus minor
	Triatriopollenites excelsus

Table 2 continued

Cluster no.	Palynomorph content
Cluster 7	*Tricolporopollenites cingulum*
	Tricolpopollenites liblarensis/quisqualis
Cluster 8	*Plicatopollis* spp.

The resulting frequency graphs of these clusters were used as the database for the time series analyses (see Fig. 9)

producers. Thus, despite the rarity of their pollen, Hydrocharitaceae at Messel probably occupied shoreline habitats similar to their recent counterparts in the tropics and subtropics.

Other taxa such as *Tricolporopollenites messelensis* and *T. solé de portai* also show their peak abundance in the lower part of the diagram. Thiele-Pfeiffer (1988) recognized similarities of *T. messelensis* with the pollen of *Ligustrum japonicum* (Oleaceae) and *Euodia roxburghiana* (Rutaceae), while *T. solé de portai* shows some affinities to pollen of certain extant Rosaceae and Anacardiaceae (Thiele-Pfeiffer 1988). But these assignments remain somewhat uncertain.

Various species of *Plicatopollis* (Juglandaceae, walnut family) dominate with values of >50% in some samples, but their frequency shows strong fluctuations. The other two dominant taxa in Messel are *Tricolpopollenites liblarensis* and *Tricolporopollenites cingulum*. Both taxa include pollen of more than one natural taxon. While *T. cingulum* is generally attributed to the Fagaceae (beech family), the affinity of *T. liblarensis* is uncertain with Fagaceae, legumes (Fabaceae), Combretaceae or Verbenaceae being possible sources (Stuchlik 1994).

Some other taxa which occur throughout the entire Middle Messel Formation are frequent in zone 1, but very rare in the two succeeding zones, e.g. *Pityosporites labdacus* (Pinaceae) and *Platycaryapollenites* (Juglandaceae, walnut family).

Zone 2 (74.08–66.08 m)

Zone 2 includes 41 samples and covers a time interval of approximately 56 kyr. The freshwater dinoflagellate cysts of *Messelodinium* continue to occur frequently with a conspicuous peak of >80% at 71.67 m depth. But they almost disappear at the top of zone 2 with only rare specimens in the succeeding zones.

The pollen spectra of zone 2 differ from those of zone 1 mainly in some obvious frequency changes, such as a decrease in *Pityosporites labdacus* (Pinaceae) and *Platycaryapollenites* (Juglandaceae). *Leiotriletes* spp. and *Tricolporopollenites solé de portai* are still frequent throughout. In contrast,
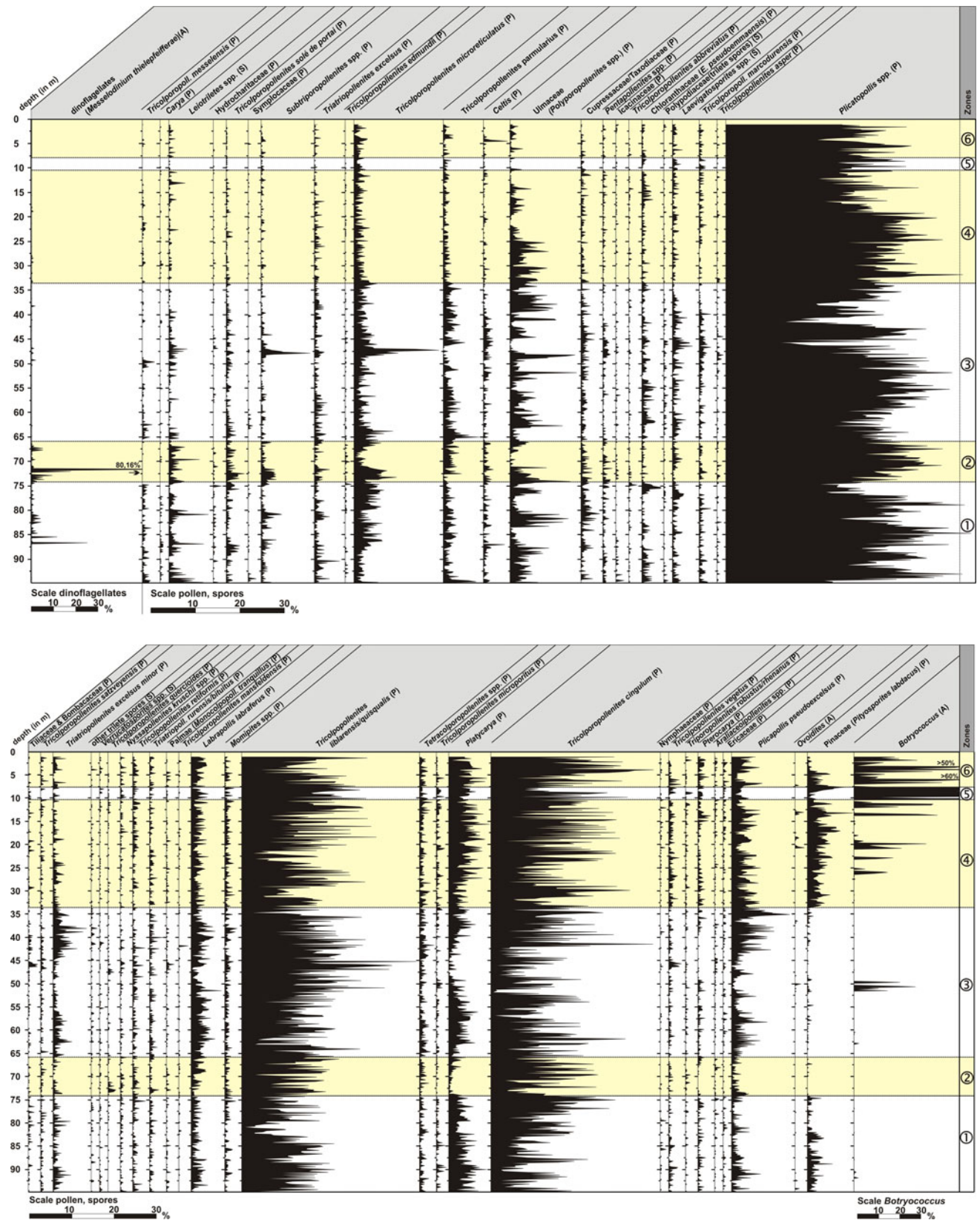
Fig. 4 *Part 1, part 2* Pollen diagram of upper part of lake sediments in Messel (climax phase, Middle Messel Formation). The diagram shows six palynological zones, derived from OSIC (optimal splitting by information content, see text). Abbreviations behind the species names: (A) alga, (P) pollen, (S) spore

taxa like *Tricolporopollenites microreticulatus* (Oleaceae, olive family; Lenz 2005) and *Polyporopollenites* spp. (Ulmaceae, elm family; Lenz et al. 2007a) show remarkable fluctuations within zone 2 including the highest values for the Middle Messel Formation.

Zone 3 (65.88–33.68 m)

Zone 3 includes 162 samples and covers a time interval of approximately 225 kyr. This zone is characterized by distinct changes in the palynomorph spectrum particularly with regard to the algal population in the lake. *Messelodinium* almost disappears, but the few remaining specimens document that the respective dinoflagellates were still present, perhaps even common as motile stages but with a low rate of cyst formation (Lenz et al. 2007b). On the other hand, this zone includes the first mass occurrence of the green alga *Botryococcus* with 15–30% in a short interval between 51.50 and 49.70 m covering a period of about 12,500 years.

The temporary occurrence of *Botryococcus* in zone 3 is associated with temporary but significant changes among other palynomorphs. Although occasional short-term mass occurrences of *Polyporopollenites* spp. (Ulmaceae) have already been observed in zones 1 and 2, they show a pronounced peak at 48.28 m. Subsequently, *Subtriporopollenites* spp. (47.88 m) and *Tricolporopollenites microreticulatus* (47.28 m) show a short-term maximum, followed by a temporary decrease in *Plicatopollis* spp. (45.68 m).

Within about 40,000 years after the first occurrence of *Botryococcus,* notable changes in the lake and the surrounding vegetation are apparent and sustained. For example, there is a remarkable decrease in the frequency of the spores *Leiotriletes* spp. and *Laevigatosporites* spp. Other taxa like *Triatriopollenites excelsus minor* (Myricaceae/Juglandaceae group) and *Plicapollis pseudoexcelsus* (Juglandaceae?) show increasing values at 45 m. Since *Platycaryapollenites* is again represented by high values, *Platycarya* can now be considered as permanently established in the vegetation from about 45 m upward.

Zone 4 (33.48–10.48 m)

Zone 4 includes 115 samples and covers a period of approximately 160 kyr. Most obvious is the sudden recurrence of the pinaceous pollen *Pityosporites labdacus.* Noteworthy, too, is the regular occurrence of *Botryococcus* with up to 40% in a number of samples.

Apart from that only moderate changes can be recognized in comparison with zone 3. The long-term trends in frequency distribution of some palynomorphs, which started in zone 3, continue in zone 4.

Zone 5 (10.28–7.88 m)

With only 13 samples and a time interval of only 16,800 years, this zone is considerably shorter than the previous zones and characterized by striking peak abundances of *Botryococcus* (coccal green algae) dominating the samples with up to 280% (relative to the total number of pollen and spores).

Zone 6 (7.68–1.09 m)

Zone 6 represents the uppermost part of the Middle Messel Formation in the core and includes 33 samples covering a period of approximately 45.000 years. *Botryococcus* is still very common dropping somewhat to 61% from its peak in zone 5. *Plicatopollis* still dominates, but on a lower level than in zones 1–3. In contrast, *Tricolporopollenites cingulum* reaches peak abundance.

Discussion

A stable paratropical climax vegetation typical for inland sites of Western and Central Europe flourished in the vicinity of Messel during the Middle Eocene greenhouse phase at the time of the eruption (Mai 1981, 1995; Schaarschmidt 1988). After severe disturbance by the eruption and a recovery phase represented by the Lower Messel Formation (Lenz et al. 2007a), the same climax vegetation was re-established without changes in floristic composition. The stability of the climax vegetation is confirmed by the fact that no first or last appearances of pollen taxa have been observed in our study during the 640 kyr represented by the Middle Messel Formation. By means of time series analyses, however, we are able to show that frequency fluctuations of individual elements occurred probably in response to orbital cycles within this period of the Middle Eocene greenhouse phase. In addition, a gradual quantitative change in the palynomorph spectrum of the climax vegetation throughout the section may be noted.

Detrended correspondence analysis (DCA) has been applied in order to detect long-term palaeoecological trends and clearly shows a successive change in the composition of vegetation and phytoplankton (Figs. 5, 6, 7). In the scatter plot of the first two axes from the DCA, showing the arrangement of samples, the six palynological zones are contoured (Fig. 5). The first two axes reflect only 17.5% of the total deviation (CA 1: 11.50, CA 2: 6.0), a relatively low value considering the great number of taxa with 0% values and the relatively small changes in the composition of the data set.

There is a clear separation between samples from the first two zones on the left side of the diagram with negative or low positive values and samples from zones 4 to 6 on the

Fig. 5 Scatter plot of the first two axes from a detrended correspondence analysis (DCA), showing the arrangement of samples. The different symbols represent samples from the six palynological zones shown in Fig. 4 derived by the broken stick method (see text)
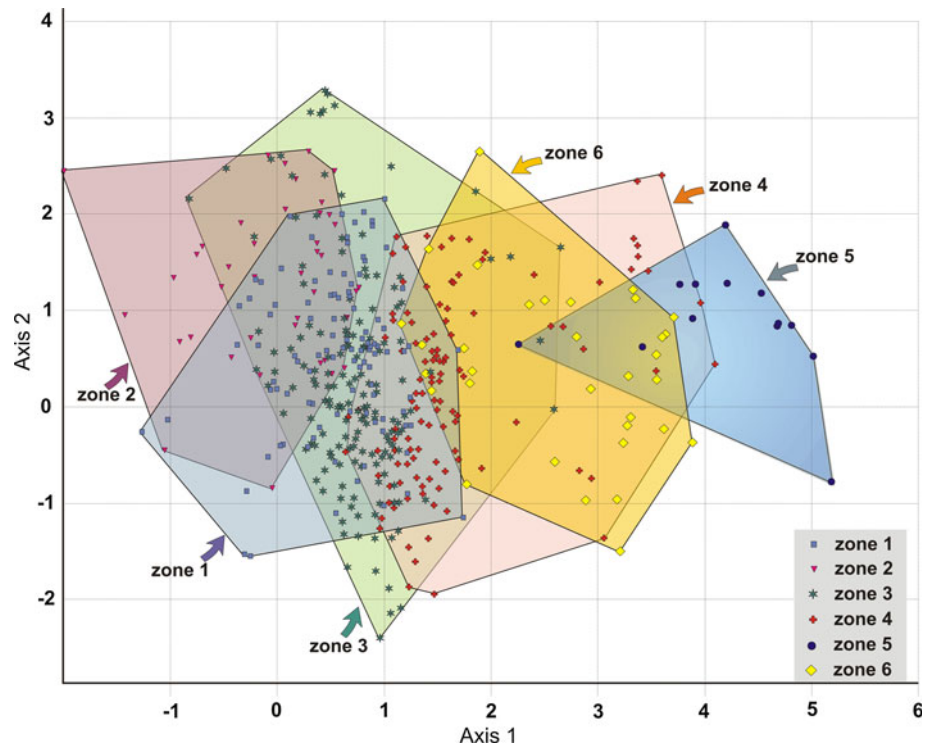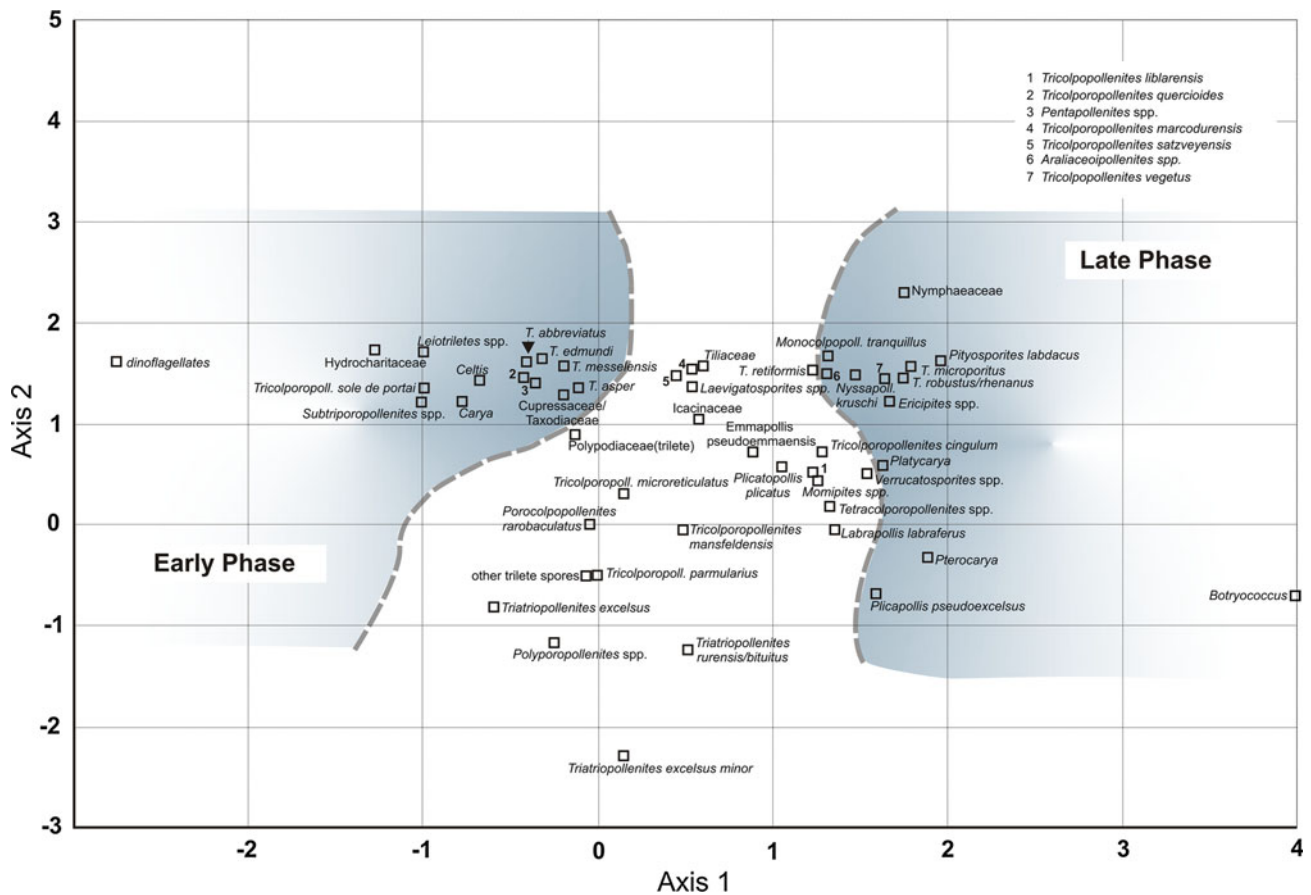
Fig. 6 Plot of the first two axes from a detrended correspondence analysis (*DCA*), showing the arrangement of palynological zones 1–6. The *arrows* in **b** reveal the temporal succession of these zones. This demonstrates that there is a gradual change in the general composition of the climax vegetation between an early phase (*zones 1, 2*) and a late phase of the Middle Messel Formation (*zones 4, 5* and *6*). The *dashed line* bordered the intermediate phase, in which *zone 3* and the zones of the early and late phases overlap
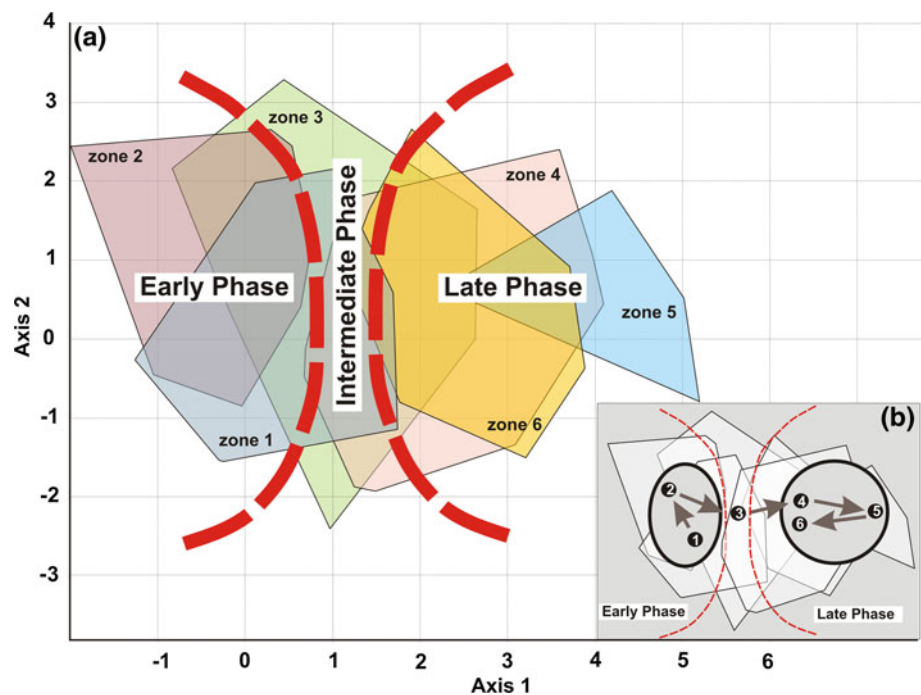
right side with positive values above 1. There is only a small gap between the two groups located well within zone 3. Thus, floral development within the Middle Messel Formation can be divided into three phases: The first axis clearly separates an early phase (zones 1, 2) within the Middle Messel Formation from a late phase (zones 4, 5, 6) with an intermediate phase (zone 3) in between,

emphasizing that changes in the composition of the vegetation were gradual (Fig. 6).

Correspondingly, the DCA plot of taxa in Fig. 7 shows a group of palynomorphs on the negative side of axis 1 which were only abundant during the early phase. Especially, the dinocyst *Messelodinium* shows a distinct negative value. On the other hand, taxa particularly occurring in the late

Fig. 7 Scatter plot of the first two axes from a detrended correspondence analysis (*DCA*), showing the arrangement of taxa. Taxa on the left side, highlighted in *grey*, show their peak abundance in the lower part of the Middle Messel Formation (early phase), taxa on the right side, also highlighted in *grey*, in the upper part (late phase)

phase are located on the positive side of axis 1, on which the value of *Botryococcus* is rather excentric.

In the pollen assemblages of the Middle Messel Formation, the Juglandaceae (walnut family) are particularly well represented by a total of 14 different pollen taxa (Table 1), primarily by *Plicatopollis* spp., but pollen of *Platycarya, Carya, Engelhardia* (*Momipites* spp.) and *Subtriporopollenites* spp. are also frequent. Together with an abundant macrofossil record (Wilde 1989, 2004), this is proof of the dominant role of Juglandaceae in the regional flora during the Middle Eocene. A considerable diversity of juglandaceous pollen taxa is also well known from other Palaeogene localities especially in North America, e.g. from the Palaeocene/Eocene boundary section in the Williston Basin in North Dakota, USA (Harrington et al. 2005) and the latest Palaeocene in the US Gulf Coast region (Frederiksen 1998, Harrington and Kemp 2001). The first occurrences of *Plicatopollis* and *Platycarya-pollenites* probably marked the transition from the latest Palaeocene to the Early Eocene and seem to be the main basis for the proposed floral turnover within the PETM of the US Gulf Coast region.

Two other main elements, *Tricolpopollenites liblarensis* and *Tricolporopollenites cingulum*, dominate the pollen spectra with 50–70%. Although *T. cingulum* can be attributed to the Fagaceae, macroscopic remains of Fagaceae, in contrast to the Juglandaceae, have never been found at Messel (Wilde 1989, 2004). Since the specific taphonomic scenario of maar lakes precludes long-distance transport at Messel for most plant parts, except for pollen, the habitat of the Fagaceae is considered to have been located outside the narrow catchment area of the lake (e.g. Spicer and Greer 1986, Ferguson 1993). A similar relationship may be assumed for *Tricolpopollenites liblarensis* and the site of its parent plants. Therefore, the frequency of *T. liblarensis* and *T. cingulum* is assumed to be least controlled by local effects and to best reflect the true zonal vegetation. The two taxa are closely clustered in the centre of the DCA plot together with *Plicatopollis* spp. and therefore appear to be ideally suited for time series analyses.

Goth (1990) has shown that the coccal green alga *Tetraedron minimum* is the most common element of the phytoplankton in the oil shale with *Botryococcus* and the central diatom *Melosira* as additional primary producers.

However, since *Tetraedron* is lost in our slides by screening due to its small size of $<10\mu$, and *Melosira* is only represented by imprints in the organic matter of the oil shale, their distribution cannot be addressed here.

Early phase (Zones 1 and 2)

Palynological zones 1 and 2 represent the early phase of the Middle Messel Formation between 94 and 66 m which is characterized by two elements: the phytoplankton within the lake and the semiaquatic to terrestrial vegetation immediately surrounding it.

Mass occurrences of the dinocyst species *Messelodinium thielepfeifferae* recorded in the Lower Messel Formation by Lenz et al. (2007a, b) are thought to have resulted from indigenous monospecific populations of freshwater dinoflagellates. They apparently favoured the holomictic conditions during the initial lake phase and quickly declined with the onset of meromictic conditions near the top of the Lower Messel Formation. They return, however, with relatively high frequencies in zones 1 and 2 of the Middle Messel Formation despite the predominance of meromictic conditions. In this early phase, primary production in Lake Messel may have been fuelled by nutrient input from still somewhat unstable crater walls to produce the mass occurrences of freshwater dinoflagellate cysts in some samples. Similarly, Köhler and Clausing (2000) considered ash fall as a source for nutrient concentration in the Oligocene Enspel lake, Westerwald, Germany, followed by acme occurrences of freshwater dinoflagellate cysts.

A pronounced peak of *M. thielepfeifferae* with more than 80% at 71.67 m is associated with a redeposit between 71.50 and 71.80 m (Fig. 3). In this case, it is conceivable that cysts originally concentrated by wave and wind drift along the shore were transported by slumping to the lake floor. This process has also been invoked to explain similar accumulations of the green alga *Botryococcus* in the slightly younger Eckfeld maar lake (Nickel 1996).

Among the terrestrial plants those dependent on aquatic habitats and moist substrates are best represented in the assemblages of zones 1 and 2. The DCA plot shows the aquatic Hydrocharitaceae and ferns of the family Schizaeaceae with various species of *Leiotriletes* at the left side of the diagram (Fig. 7). But an ecological interpretation of *Leiotriletes* is equivocal since spores of this type occur not only in *Lygodium* (Schizaeaceae) but also in the families Dicksoniaceae and Matoniaceae (Collinson 2001). Nevertheless, the distribution of Hydrocharitaceae pollen and fern spores indicates extended areas of shallow water and herbaceous swamps around the lake at this early stage of the Middle Messel Formation. This was probably caused by higher lake levels allowing the spread of aquatic plants and fern flats.

The event bed separating the Lower from the Middle Messel Formation (Felder and Harms 2004) indicates a major collapse of the crater walls at the beginning of the Middle Messel Formation, leaving barren areas to be recolonized. Therefore, at the beginning of this early phase the pollen spectra are reminiscent of those from the initial recolonization, especially with regard to the great number and high diversity of fern spores, including *Leiotriletes* (Lenz et al. 2007a). Schizaeaceae such as *Lygodium* producing *Leiotriletes*-type spores are known today from volcanic terrains where they colonize open and disturbed habitats (Collinson 2002).

Open areas on newly collapsed slopes allowed pollen of plants from more distant sources to reach the lake surface. This could explain the relatively high values for pollen of Pinaceae (*Pityosporites labdacus*) in zone 1. Later, the complete recolonization of the crater slopes by a dense climax vegetation has statistically suppressed the input of airborne pollen such as *P. labdacus* in the succeeding zones 2 and 3.

Tricolporopollenites messelensis and *T. solé de portai* which reach their peaks in zones 1 and 2 were found in similar quantities in the Lower Messel Formation. They have been assigned to the Oleaceae/Rutaceae and Rosaceae/Anacardiaceae, respectively (Thiele-Pfeiffer 1988), which may, therefore, be considered as part of a pioneering vegetation.

Intermediate phase (Zone 3)

Zone 3 represents an intermediate phase which shows considerable overlap with the zones of the early and the late phase in the DCA plots of samples (Figs. 5, 6). The overlap is most pronounced with zones 1 and 4, indicating that zone 3 shares characteristics with the "wet" zone 1 and anticipates to some extent the drier conditions of the late phase. Similarities with zone 1 are mainly due to a resedimentation event in the middle of zone 3 which is reflected by a succession of peaks of pollen considered to represent a pioneering vegetation (Lenz et al. 2007a). After a first pronounced but isolated peak of *Botryococcus*, peaks of *Tricolporopollenites messelensis*, pollen of Ulmaceae, *Subtriporopollenites* spp., *Tricolpopollenites microreticulatus* together with *Leiotriletes* spp., and *Laevigatosporites* spp. follow each other. This succession is observed across a core interval of a little more than 4 m representing a time slice of approximately 30,000–32,000 years. It is largely responsible for the strong midterm signal in the wavelet time–frequency spectrum which is probably associated with the 400 kyr Milankovitch frequency band occurring just once within our section (see "Trends and cycles"). Higher up in the section, *Plicapollis pseudoexcelsus* and *Tricolporopollenites cingulum* are clearly more frequent

and remain at relatively high levels throughout the late phase, indicating that this event was somehow coupled with lasting effects on the regional vegetation and climate, including a sustained trend towards a reduction in humidity.

Late phase (Zones 4, 5 and 6)

Since *Pinus* is more tolerant to aridity and well-drained soils than most of the plants known as components of the regional climax forest around the Messel site, the sharp increase in pinaceous pollen (*Pityosporites labdacus*) suggests that the climate became drier near the end of the Middle Messel Formation. Plants especially sensitive to more humid conditions were suppressed by a spread of Pinaceae in the vegetation. The same is indicated by a considerable decline of fern spores, especially *Leiotriletes* spp. and *Laevigatosporites* spp.

For the late phase, a fundamental change in the phytoplankton population of the Messel lake is indicated by mass occurrences of *Botryococcus* especially in zones 5 and 6. Today, *Botryococcus* has an almost cosmopolitan distribution ranging from the tropics to sub-arctic climates. It predominantly occurs in freshwater lakes (Traverse 1992; Taylor et al. 1998) but also tolerates weakly saline conditions (De Deckker 1988; Batten 1996). *Botryococcus* is common across a wide range of trophic conditions (Ruttner 1952; Round and Brook 1959; Round 1981; Komárek and Marvan 1992; Tyson 1995; Batten 1996), including slightly alkaline lakes (Wetzel 1983, De Deckker 1988). Obviously tolerating quite different climatic conditions, optimal conditions for its growth have been recorded from shallow lakes at low precipitation (Guy-Ohlson 1992; Batten and Grenfell 1996).

Mass occurrences of *Botryococcus* at Messel can therefore be considered to reflect long-term changes in water chemistry which were connected with a change from more humid conditions with higher water levels at the beginning of the Middle Messel Formation to raised evaporation and, consequently, lower water levels. This may have been coupled with an extension of shallow water areas as indicated by the more common occurrence of Nymphaeaceae (water lily family) pollen in this late phase. In view of the probable terrestrialization in the Upper Messel Formation, it is interesting to note that mass occurrences of *Botryococcus* in combination with pollen of *Nymphaea* have been commonly found at marl/lignite boundaries in Neogene lake basins of Greece (Riegel et al. 1995).

Trends and cycles

The three phases of the Middle Messel Formation reflect long-term changes in the vegetation around Lake Messel and the hydrobiology within the lake during the early Middle Eocene. The pollen diagram furthermore shows a general trend from humid to somewhat drier conditions which are overprinted by fluctuations in the frequency of individual taxa, in particular, of the dominant elements such as *Plicatopollis* spp., *Tricolpopollenites liblarensis* and *Tricolporopollenites cingulum* which appear to be independent of the zonation (Fig. 4). In order to test whether these fluctuations follow regular patterns caused by cyclic fluctuations in the pollen rain due to climatic variations, time series analyses have been performed.

Since most Eocene pollen can only be assigned to family level, palaeoecological interpretations are restricted in terms of extant species or genera. Therefore, we use clusters in which taxa with similar climatic and ecologic affinities are grouped (Figs. 8, 9). They mainly consist of the pollen rain of the regional Middle Eocene paratropical climax forest dominated by the pollen of Juglandaceae (e.g. *Plicatopollis* spp.) and Fagaceae (*Tricolporopollenites cingulum*), respectively, Leguminosae (*Tricolpopollenites liblarensis*) but include some influx from seral stages immediately surrounding Lake Messel (Thiele-Pfeiffer 1988; Wilde 2004; Lenz et al. 2007a). The former are mainly combined in clusters 1 and 6–8, the latter concentrated in clusters 2 and 3 (Table 2).

Since lamination of the oil shale is highly uniform, the pollen assemblages obviously were not influenced by changes in taphonomic conditions within the lake or surface runoff from outside. Therefore, we conclude that the frequency distribution of these clusters reflects shifts in the composition of the paratropical climax forest which were essentially induced by climate variability, too moderate, however, to affect the character of the lake sediments.

These shifts especially affected the relative proportion of Fagaceae (*Tricolpopollenites liblarensis, Tricolporopollenites cingulum*) and Juglandaceae (mainly *Plicatopollis* spp.) in the regional vegetation as well as seral stages accompanying the lake shore, including aquatic and hydrophilous plants (e.g. Nymphaeaceae and Restionaceae), heliophytes (e.g. lianas of the families Icacinaceae and Araliaceae) and various arborescent and shrubby pioneers (palms, Ulmaceae, Oleaceae). The results of both time series analyses, wavelet transform and spectral analysis, for the percentage values of 4 selected clusters are shown in Figs. 10, 11, 12 and 13 (clusters 1, 2, 5 and 8). The analyses of the other clusters are attached as electronic supplementary material. They clearly show that the vertical distribution of wavelet power signals corresponds to that of the clusters throughout our section. Cluster 1 shows strong signals in the upper part of the section (Fig. 10), cluster 5, to the contrary, only in the lower part (Fig. 12). Only the clusters 7 and 8 which are formed by pollen occurring in mass abundance show signals continuous throughout the section (Fig. 13).
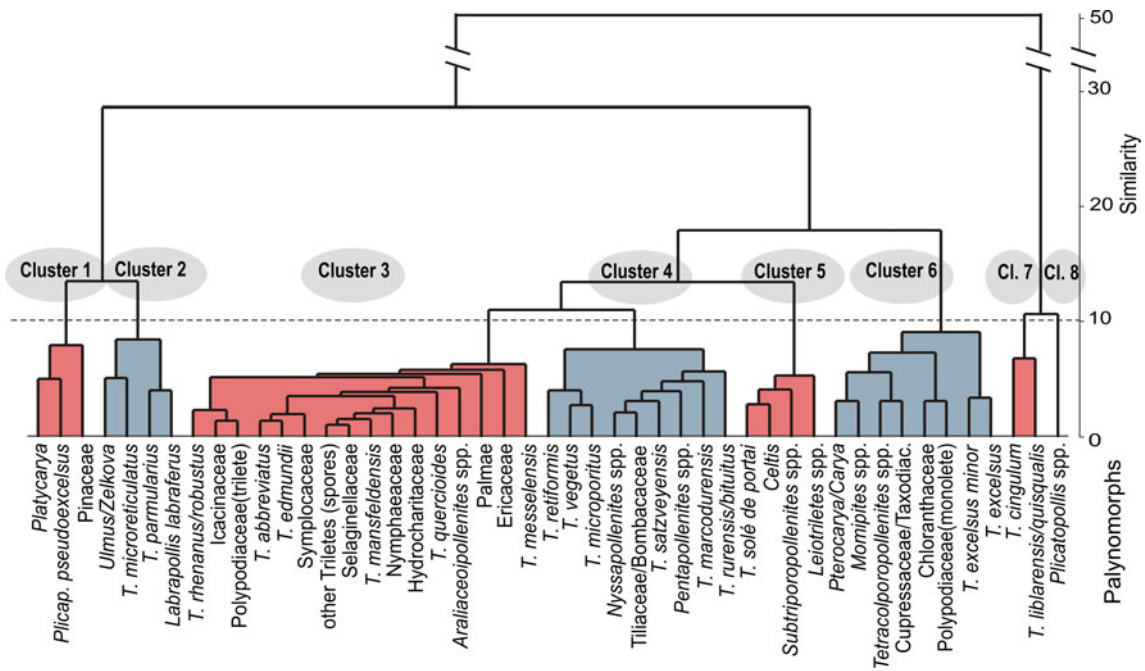
Fig. 8 Dendrogram of the cluster analysis of 47 palynomorphs or groups of palynomorphs from the Middle Messel Formation (Ward's method, 458 samples)
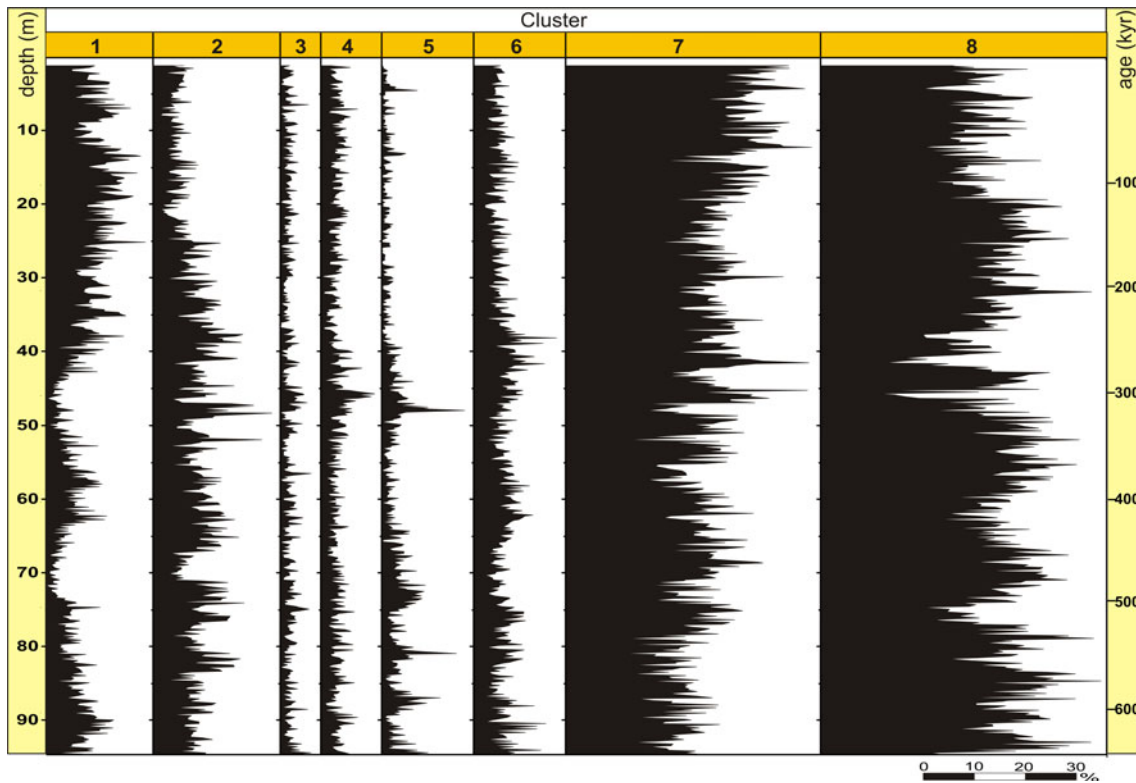
Fig. 9 Percentage diagram of the eight clusters from the cluster analysis of the Middle Messel Formation (see Fig. 8). Also included is an estimated age/depth scale based on a calculated sedimentation rate of 0.14 mm/year. The sampling interval represents approximately 1 sample every 1.4 kyr

All of the clusters show distinct signals within the range of the Milankovitch frequency band. Most pronounced are the signals for obliquity (about 40–45 kyr) and precession (about 23 kyr). In clusters 1, 2 and 8 (Figs. 10, 11 and 13), it is even possible to distinguish between a long precession in the range between 22 and 25 kyr and a short precession between 16 and 19 kyr. Signals in the range of short eccentricity (about 100 kyr) cannot always be clearly recognized. However, wavelets in the range between 64 and 128 kyr show signals sufficiently distinct to assume affinities to the eccentricity cycle. Obviously, eccentricity cannot be clearly distinguished since the cycle was

repeated only six times in our section, while obliquity and precession cycles recurred at least 16, respectively, 30 times. Additional spectral analyses (RedFit) confirm the statistical significance of the individual signals for the Milankovitch frequency range (Figs. 10, 11, 12, 13).

The time interval of 1.4 kyr calculated for the sample distance of 20 cm does not allow for sufficient resolution of periods below 4 kyr. Yet, there are significant sub-Milankovitch signals of around 12 and 6 kyr which are probably linear harmonics of the precession cycle (Berger and Loutre 1997; Berger et al. 2006). Cyclicities beyond the Milankovitch frequency band and their influence on the
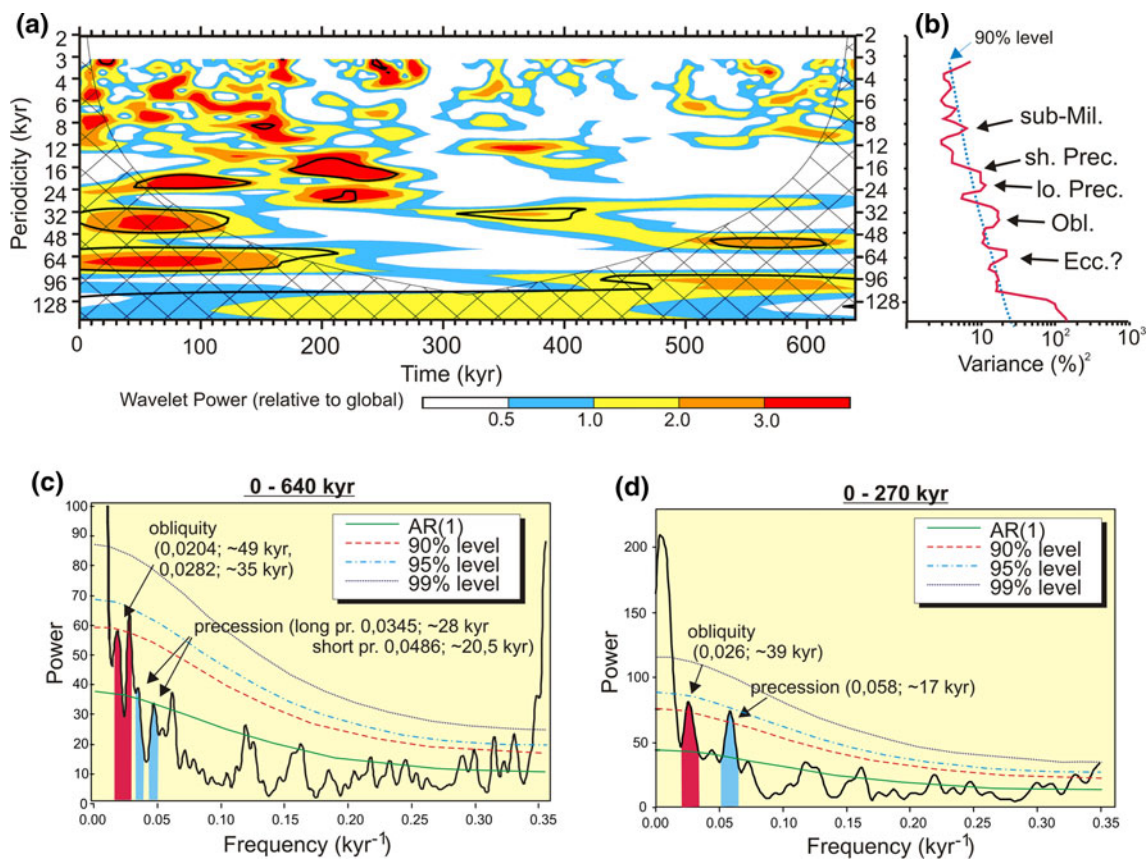
Fig. 10 Times series analyses of cluster 1. **a** continuous wavelet time–frequency spectrum (Morlet wavelets) of total percentage curve of cluster 1. The wavelet power at each period is normalized by the global wavelet spectrum. To reduce wraparound effects, the time series is padded with zeros. The *hatched areas* show regions in which edge effects caused by zero padding are significant. *Black contours* correspond to power which is significant at 90% confidence level, using a *white-noise background* spectrum. The *red* and *orange coloured areas* indicate strong effects of a cycle at a certain time interval, while *blue* and *white areas* represent little or no effect. In the time interval of 0–270 kyr, pronounced signals of precession (21 kyr), at the time interval 170–270 kyr even short precession (∼17 kyr) and long precession (∼24 kyr), and obliquity (40–44 kyr) are visible. An eccentricity signal at 100 kyr is not significant, but sub-Milankovitch signals around 6–12 kyr are indicated. **b** Global wavelet spectrum. The *dashed line* shows the corresponding 90% significance level. Significant peaks are labelled with their correlation

to orbital periods. Analyses in **b** and **c** were undertaken using interactive software available at http://atoc.colorado.edu/research/wavelets/ by using the methods of Torrence and Compo (1998). **c** Bias-corrected spectrum of the total percentage curve of cluster 1 for the time interval 0–640 kyr, computed using a FFT. The spectral estimate represents the average over seven segments with 50% overlap and without tapering (*rectangular window*), and 90, 95 and 99% confidence levels are shown. Detectable spectral peaks within the Milankovitch frequency band are labelled with their periods in kyr. Only a double peak within the obliquity frequency band is significant at the 90% level. **d** Bias-corrected spectrum for the time interval 0–270 kyr, where the wavelet time–frequency spectrum (**a**) shows the strongest signals. The spectral estimate represents the average over five segments with 50% overlap and without tapering (*rectangular window*). A conspicuous increase in the significance for obliquity and precession is noticeable. The spectra in **c** and **d** were calculated with software REDFIT 3.8
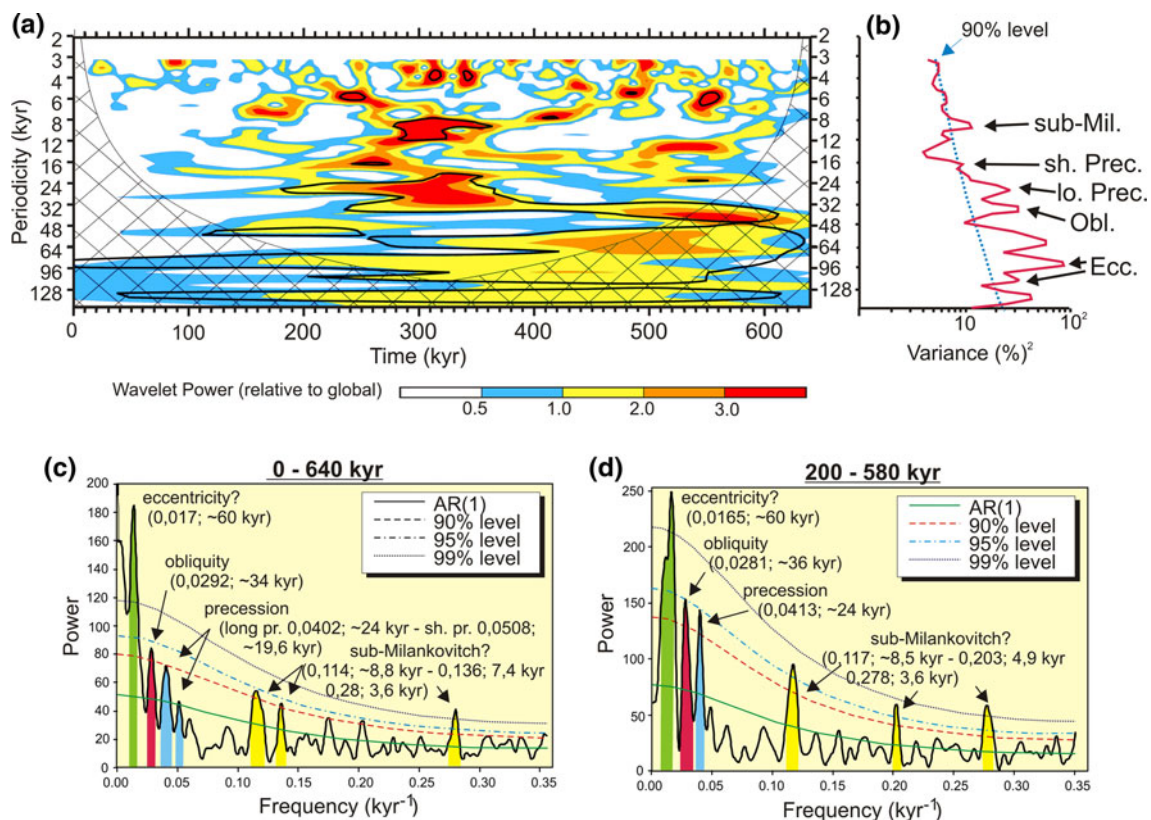
Fig. 11 Times series analyses of cluster 2. **a** continuous wavelet time–frequency spectrum (Morlet wavelets) of total percentage curve of cluster 2. In the time interval of 200–580 kyr, pronounced signals of precession ($\sim$24 kyr) and obliquity ($\sim$40 kyr) are visible. A possible eccentricity between 60 and 100 kyr and significant sub-Milankovitch signals around 6–12 kyr are indicated. **b** Global wavelet spectrum. **c** Bias-corrected spectrum of the total percentage curve of cluster 2 for the time interval 0–640 kyr (average over seven segments with 50%

overlap, rectangular window). Precession, obliquity and three sub-Milankovitch signals are significant at the 90% level. **d** Bias-corrected spectrum for the time interval 200–580 kyr, where the wavelet time–frequency spectrum (**a**) shows the strongest signals (average over four segments with 50% overlap, *rectangular window*). A conspicuous increase up to the 95% level of the significance for all Milankovitch and sub-Milankovitch cycles of **c** is noticeable. For further information, see the caption of Fig. 10

high-latitude and East African climate are known for the tropical Pleistocene (Trauth et al. 2003; Turney et al. 2004). But, sub-Milankovitch cyclicity in the Messel oil shale is part of an ongoing detailed study.

Our data show that the distribution of palynomorphs as combined by cluster analysis can be related to Milankovitch cyclicity in the short eccentricity, obliquity and long and short precession frequency. Minor deviations from Quaternary frequencies may be due to chaotic orbital evolution (Varadi et al. 2003; Laskar et al. 2004) or intermittent irregularities in the rate of sedimentation.

The strong signals displayed about midterm between 250 and 350 kyr (Figs. 10, 11, 12, 13) by all clusters except cluster 1 may be due to the superposition of several cycles in the 400-kyr-long eccentricity range which must be recorded once within the 640 kyr of our section. The midterm signals are most pronounced in cluster 5 (Fig. 12), but also significant in clusters 2 (Fig. 11) and 3. The ecological significance of cluster 5 is difficult to assess. Cluster 2, however, includes mainly elements considered to

represent terminal seral stages, e.g. Ulmaceae and *Tricolporopollenites microreticulatus*, while cluster 3 includes most of the aquatic and hydrophilous elements in our assemblage (Fig. 8). Thus, this midterm signal may reflect a transient climatic disturbance including an increase in precipitation and, possibly, raised lake levels triggered by the 400-kyr eccentricity band. With some delay, this was succeeded by the most lasting and pronounced change of vegetation involving an increase in pollen of Pinaceae and some Juglandaceae combined in cluster 1 (*Pityosporites* sp., *Plicapollis pseudoexcelsus*, *Platycaryapollenites* sp.) due, perhaps, to a greater expanse of drier habitats in the pollen source area.

Conclusions

Our palynological analysis of the oil shale of the Middle Messel Formation sheds new light on how the Middle Eocene paratropical climax vegetation and the aquatic
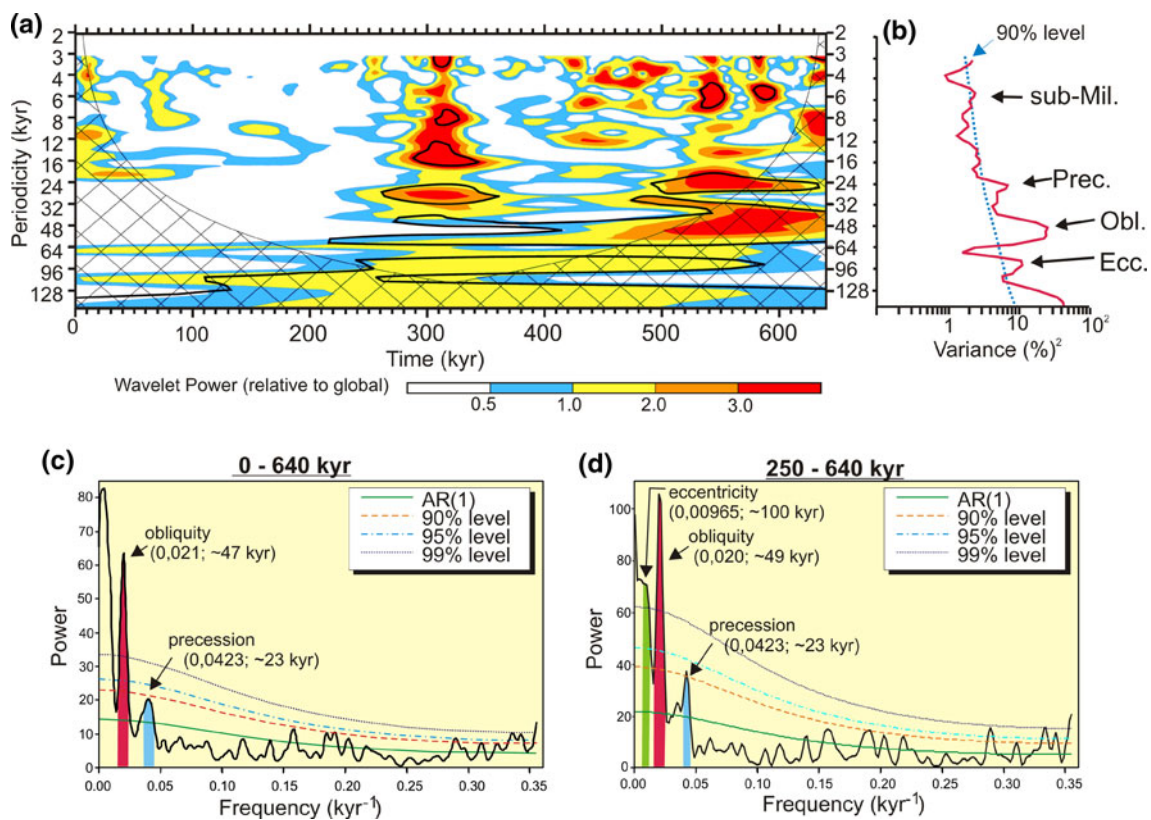
Fig. 12 Times series analyses of cluster 5. **a** continuous wavelet time–frequency spectrum (Morlet wavelets) of total percentage curve of cluster 5. In the time interval of 250–640 kyr, pronounced signals of precession (∼24 kyr), in the time interval 250–350 kyr even short precession (∼17 kyr) and long precession (∼24 kyr), and obliquity (∼40 kyr) are visible. A possible eccentricity at 96 kyr and significant sub-Milankovitch signals around 5–8 kyr are indicated. **b** Global wavelet spectrum. **c** Bias-corrected spectrum of the total percentage curve of cluster 5 for the time interval 0–640 kyr (average

over seven segments with 50% overlap, *rectangular window*). A strong obliquity signal is significant at the 99% level. The precession peak is not significant for this time interval. **d** Bias-corrected spectrum for the time interval 250–640 kyr, where the wavelet time–frequency spectrum (**a**) shows the strongest signals (average over four segments with 50% overlap, *rectangular window*). A conspicuous increase in the significance for obliquity and precession is noticeable. The eccentricity signal is indicated. For further information, see the caption of Fig. 10

environment of the Messel lake were affected by climate variability.

Basically, a gradual change of climate took place during the time of the Middle Messel Formation. In the early phase, the vegetation included a high proportion of plants associated with "wet" and humid conditions, mainly raised water levels and higher rainfall. After a transitional period, distinctly less humid conditions dominated in the late phase. The first axis of the DCA separates the vegetation of more humid conditions from the vegetation of less humid conditions (Fig. 7). This suggests that vegetation changes within the Middle Messel Formation were mainly controlled by precipitation and humidity. At the same time, there is no palynological evidence of sustained changes in temperature.

In addition to their impact on vegetation, changes in precipitation also influenced the water chemistry (acidity, nutrient supply) of Lake Messel. Although important

primary producers such as the green alga *Tetraedron minimum* and the diatom *Melosira* (Goth 1990) were lost by palynological preparation, quantitative data on the distribution of freshwater dinoflagellate cysts and *Botryococcus* can be used for ecological considerations. In the early phase, dinoflagellate blooms may still have been driven by nutrient input from the somewhat unstable crater wall. The sudden increase in *Botryococcus* in the uppermost 25 m of the core indicates a substantial change in water chemistry towards increased alkalinity favoured by *Botryococcus* (Wetzel 1983; Zippi 1998) and possibly due to an increase in evaporation during the late phase of the lake (Wilde et al. 1993; Lenz et al. 2007b).

Our time series analyses clearly show cyclic variation in the quantitative composition of palynomorph assemblages during a 640-kyr interval of the Middle Eocene as represented by 91.6 m of laminated oil shale of the Middle Messel Formation. The observed cycles closely correspond
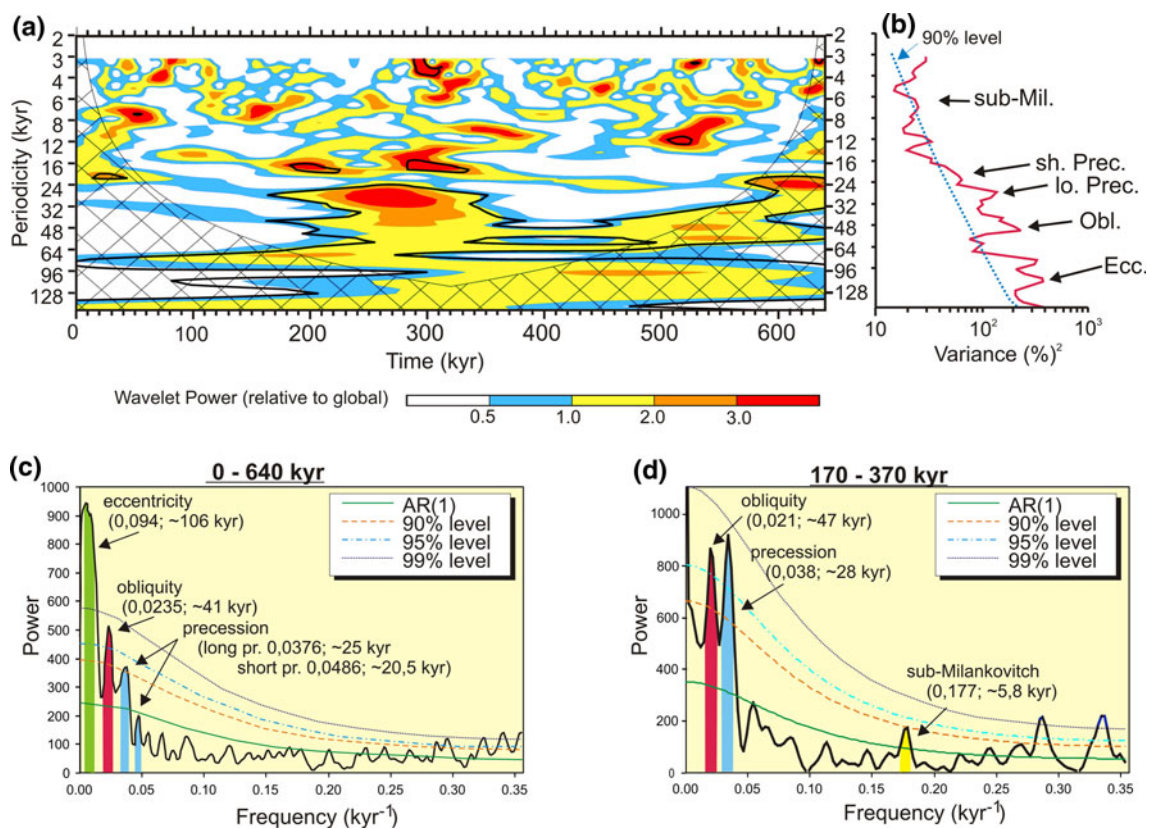
Fig. 13 Times series analyses of cluster 8. **a** continuous wavelet time–frequency spectrum (Morlet wavelets) of percentage curve of *Plicatopollis* spp. More or less pronounced signals occur throughout the entire time interval 0–640 kyr. In this interval, orbital periods of precession (∼21 kyr) and obliquity (∼45 kyr) are visible. A possible eccentricity at 96 kyr is indicated. **b** Global wavelet spectrum. **c** Bias-corrected spectrum of the percentage curve of C *Plicatopollis* spp. for the time interval 0–640 kyr (average over seven segments with 50% overlap, *rectangular window*). Signals for eccentricity, obliquity and precession are significant at the 90 or 95% level. **d** Bias-corrected spectrum for the time interval 170–370 kyr, where the wavelet time–frequency spectrum (**a**) shows pronounced signals (average over three segments with 50% overlap, *rectangular window*). A conspicuous increase in the significance for the obliquity and precession signals is noticeable. Because of the short-time interval, the eccentricity signal is not indicated. For further information, see the caption of Fig. 10

to the short eccentricity, obliquity and precession periods and to some extent to sub-Milankovitch periods. We, therefore, conclude that orbital forcing of climate affected the terrestrial vegetation sufficiently during the Middle Eocene greenhouse phase to be reflected in the pollen rain. However, changes in the vegetation remained transient and were restricted to the quantitative composition since no first or last appearances could be observed within the studied interval. Thus, any changes are definitely on a lower scale than those proposed for the hyperthermal events as known, e.g. from the earlier Palaeogene in North America (Wing et al. 2003; Harrington and Jaramillo 2007). According to the southern hemisphere deep sea temperature data of Zachos et al. (2001) which are commonly regarded as a standard of Cenozoic climate evolution (e.g. Sluijs et al. 2005, Jaramillo et al. 2006) and are clearly reflected by Cenozoic megafloras of Central Europe (Mosbrugger et al. 2005), the 640-kyr interval covered by our section would be located on the "slope" of gradual cooling following the Early Eocene Climatic Optimum and

predating the Middle Eocene Climatic Optimum (MECO) by about 4 Myr. However, terrestrial climates are expected to be more effectively controlled by atmospheric heat transport under the Mid-Eocene ocean/continent constellation (Bice et al. 2000) and therefore more susceptible to orbital forcing factors than it is indicated by this gradual cooling trend, with significant effects, at least, on the quantitative composition of the vegetation. While the marine isotope record (Zachos et al. 2001) as well as the analysis of Cenozoic megafloras (Mosbrugger et al. 2005) resolve only long-term climate trends, the high-resolution study of the Middle Eocene lake deposits of Messel provides evidence for superimposed orbital-scale climate variability. In particular, this concerns the role of precipitation in controlling vegetation dynamics during this climatically very stable period. In a monsoonal climate as suggested for Messel by Mai (1995) and Grein et al. (in press), orbitally controlled latitudinal shifts of continental climate belts may have caused changes in the intensity of seasonal precipitation.

Although the Cenozoic climate in Central Europe is characterized by relatively stable and high precipitation rates (>1,000 mm/a), which decreased only from the early Pleistocene onward (Mosbrugger et al. 2005), variations in humidity as a driver of vegetation changes are known from the Cenozoic. For example, palaeobotanical analyses of Early Oligocene terrestrial deposits indicate that climate variability in Central Europe during the Rupelian was predominantly governed by changes in precipitation rather than by temperature fluctuations (Pross and Schmiedl 2002, Schwarzbach 1968, Schuler 1990). The effect on precipitation of early Palaeogene hyperthermal events such as the PETM has variously been interpreted as insignificant or causing even drier conditions in part for North America (Harrington and Kemp 2001, Kraus and Riggins 2007) and seasonal extremes in Spain (Schmitz and Pujalte 2007). Our study now suggests that changes in precipitation may have led to noticeable quantitative changes in the microflora at Messel even during the generally stable phase of the Palaeogene climate.

References

Bains S, Norris RD, Corfield RM, Faul KL (2000) Termination of global warmth at the Palaeocene/Eocene boundary through productivity feedback. Nature 407:171–174

Barrett PJ (1996) Antarctic paleoenvironment through Cenozoic times: a review. Terra Ant 3:103–119

Batten DJ (1996) Palynofacies and palaeoenvironmental interpretation. In: Jansonius J, McGregor DC (eds) Palynology: principles and applications, vol. 3—New Directions, other Applications and Floral History, Am Assoc Strat Palyn Found, pp 1011–1064

Batten DJ, Grenfell HR (1996) Chapter 7D. *Botryococcus*. In: Jansonius J, McGregor DC (eds) Palynology: principles and applications, vol 1, Am Assoc Strat Palyn Found, pp 205–214

Beerling DJ, Jolley DW (1998) Fossil plants record an atmospheric $^{12}CO_2$ and temperature spike across the Palaeocene-Eocene transition in NW Europe. J Geol Soc Lond 155:591–594

Bennett KD (2005) Documentation for psimpoll 4.25 and pscomb 1.03. C programs for plotting pollen diagrams and analysing pollen data. Uppsala University, Uppsala

Berger A, Loutre MF (1997) Intertropical latitudes and precessional and half-precessional cycles. Science 287:1476–1478

Berger A, Loutre MF, Mélice JL (2006) Equatorial insolation: from precession harmonics to eccentricity frequencies Clim. Past 2:131–136

Bice KL, Scotese CR, Seidov D, Barron EJ (2000) Quantifying the role of geographic change in Cenozoic ocean heat transport using uncoupled atmosphere and ocean models. Palaeogeogr Palaeocl 161:295–310

Collinson ME (2001) Cainozoic ferns and their distribution. Brittonia 53(2):173–235

Collinson ME (2002) The ecology of Cainozoic ferns. Rev Palaeobot Palyno 119:51–68

Collinson ME, Hooker JJ, Gröcke DR (2003) Cobham lignite bed and penecontemporaneous macrofloras of Southern England: A record of vegetation and fire across palaeocene-eocene thermal maximum. Geol Soc Am Spec Pap 369:333–349

Daubechies I (1990) The wavelet transform time-frequency localization and signal analysis. IEEE T Inform Theory 36:961–1004

De Deckker P (1988) Large Australian lakes during the last 20 million years: sites for petroleum source rock or metal ore deposition, or both? In: Fleet AJ et al. (eds) Lacustrine Petroleum Source Rocks. Geol Soc Spec Publ, vol 40, pp 45–58

Dunca E, Mutvei H, Göransson P, Mörth CM, Schöne BR, Whitehouse MJ, Elfman M, Baden SP (2009) Using ocean quahog (*Artica islandica*) shells to reconstruct palaeoenvironment in Öresund, Kattegat and Skagerrak, Sweden. Int J Earth Sci 98:3–17

El Bay R, Jacoby W, Wallner H (2001) Milankovitch signals in messel "Oilshales". Kaupia 11:69–72

Felder M, Harms FJ (2004) Lithologie und genetische Interpretation der vulkano-sedimentären Ablagerungen aus der Grube Messel anhand der Forschungsbohrung Messel 2001 und weiterer Bohrungen (Eozän, Messel-Formation, Sprendlinger Horst, Südhessen). Cour For Senckenbg 252:151–206

Felder M, Harms FJ, Liebig V (2001) Lithologische Beschreibung der Forschungsbohrungen Groß-Zimmern, Prinz von Hessen und Offenthal sowie zweier Lagerstättenbohrungen bei Eppertshausen (Sprendlinger Horst, Eozän, Messel-Formation, Süd-Hessen). Geol Jb Hessen 128:29–82

Ferguson DK (1993) Plant taphonomic studies with special reference to Messel. Kaupia 2:117–126

Fischer AG (1986) Climatic rhythms recorded in strata. Annu Rev Earth Pl Sc 14:351–376

Frederiksen NO (1998) Upper Paleocene and lowermost Eocene angiosperm pollen biostratigraphy of the eastern Gulf Coast and Virginia. Micropaleontology 44(1):45–68

Gauch HG (1982) Multivariate analysis in community ecology. Cambridge University Press, New York

Goth K (1990) Der Messeler Ölschiefer–ein Algenlaminit. Cour For Senckenbg 131:1–143

Grein M, Utescher T, Wilde V, Roth-Nebelsick A. Reconstruction of the Middle Eocene climate of Messel using palaeobotanical data. Neues Jahrb Geol P-A (in press)

Guy-Ohlson D (1992) *Botryococcus* as an aid in the interpretation of palaeoenvironment and depositional processes. Rev Palaeobot Palyno 71:1–15

Hammer Ø, Harper DAT, Ryan PD (2001) PAST: Paleontological Statistics Software Package for Education and Data Analysis. Palaeontol Electron 4(1). Available via http://palaeo-electronica.org/2001_1/past/issue1_01.htm

Harms FJ (2001) Eozänzeitliche Ölschiefer-Vorkommen auf dem Sprendlinger Horst (Südhessen): ein Modell zu ihrer Entstehung. Natur Museum 131(3):86–94

Harms FJ, with contrib. of Wallner H, Jacoby WR (1999) Karte zur Verbreitung der Messel-Formation/Faltblatt Welterbe Grube Messel—Map, back side with comment. Hessisches Landesamt für Bodenforschung, Wiesbaden

Harms FJ, Nix T, Felder M (2003) Neue Darstellungen zur Geologie des Ölschiefer-Vorkommens Grube Messel. Natur Museum 133(5):140–148

Harrington GJ (2001) Impact of Paleocene/Eocene Greenhouse Warming on North American Paratropical Forests. Palaios 16:266–278

Harrington GJ, Jaramillo CA (2007) Paratropical floral extinction in the Late Palaeocene-Early Eocene. J Geol Soc Lond 164:323–332

Harrington GJ, Kemp SJ (2001) US Gulf Coast vegetation dynamics during the latest Palaeocene. Palaeogeogr Palaeocl 167:1–21

Harrington GJ, Kemp SJ, Koch PL (2004) Palaeocene–Eocene paratropical floral change in North America: responses to climate change and plant immigration. J Geol Soc Lond 161:173–184

Harrington GJ, Clechenko ER, Clay Kelly D (2005) Palynology and organic-carbon isotope ratios across a terrestrial Paleocene/Eocene boundary section in the Williston Basin, North Dakota, USA. Palaeogeogr Palaeocl 226:214–232

Herrmann M (2007) Eine palynologische Analyse der Bohrung Enspel: Rekonstruktion der Klima- und Vegetationsgeschichte im Oberoligozän. Dissertation, University of Tübingen, Available via http://deposit.ddb.de/cgi-bin/dokserv?idn=986962694. Accessed 21 Dez 2007

Hill MO, Gauch HG (1980) Detrended Correspondence analysis: an improved ordination technique. Vegetatio 42:47–58

Irion G (1977) Der eozäne See von Messel. Natur Museum 107:213–218

Jacoby W, Sebazungu E, Wallner H, Gabriel G, Pucher R (2005) Potential field data fort he Messel Pit and surroundings. Cour For Senckenbg 255:1–9

Janssen CR, Birks HJB (1994) Recurrent groups of pollen types in time. Rev Palaeobot Palyno 82:165–173

Jaramillo C, Rueda MJ, Mora G (2006) Cenozoic plant diversity in the neotropics. Science 311:1893–1896

Jiménez-Moreno G, Rodríguez-Tovar FJ, Pardo-Igúzquiza E, Fauquette S, Suc J-P, Müller P (2005) High-resolution palynological analysis in the late early-middle Micocene core from the Pannonian Basin, Hungary: climatic changes, astronomical forcing and eustatic fluctuations in the Central Paratethys. Palaeogeogr Palaeocl 216:73–97

Jiménez-Moreno G, Abdul Aziz H, Rodríguez-Tovar F, Pardo-Igúzquiza E, Suc J-P (2007) Palynological evidence for astronomical forcing in Early Miocene lacustrine deposits from Rubielos de Mora Basin (NE Spain). Palaeogeogr Palaeocl 252:601–616

Kaiser ML, Ashraf R (1974) Gewinnung und Präparation fossiler Pollen und Sporen sowie anderer Palynomorphae unter besonderer Berücksichtigung der Siebmethode. Geol Jb A 25:85–114

Kennett JP, Stott LD (1991) Abrupt deep-sea warming, palaeoceanographic changes and benthic extinctions at the end oft he Paleocene. Nature 353:225–229

Köhler J, Clausing A (2000) Taxonomy and palaeoecology of dinoflagellate cysts from Upper Oligocene freshwater sediments of lake Enspel, Westerwald area, Germany. Rev Palaeobot Palyno 112:39–49

Komárek J, Marvan P (1992) Morphological Differences in Natural Populations of the Genus Botryococcus (Clorophyceae). Arch Protistenkd 141:65–100

Kovach WL (1989) Comparisons of multivariate analytical techniques for use in pre-Quarternary plant paleoecology. Rev Palaeobot Palyno 60:255–282

Kraus MJ, Riggins S (2007) Transient drying during the Paleocene-Eocene thermal maximum (PETM): analysis of paleosols in the Bighorn Basin, Wyoming. Palaeogeogr Palaeocl 245:444–461

Krutzsch W (1992) Paläobotanische Klimagliederung des Alttertiärs (Mitteleozän bis Oberoligozän) in Mitteldeutschland und das Problem der Verknüpfung mariner und kontinentaler Gliederungen (klassische Biostratigraphienpaläobotanisch- ökologische Klimastratigraphie—Evolutionsstratigraphie der Vertebraten). Neues Jahrb Geol P-A 186(1/2):137–253

Krutzsch W (2004) Neue Untersuchungen über die präquartäre Malvaceen-Pollen aus den Unterfamilien der Tilioideae, Helicteroideae und Bombacoideae. Palaeontogr Abt B 267:67–160

Krutzsch W, Vanhoorne R (1977) Die Pollenflora von Epinois und Loksbergen in Belgien. Palaeontogr Abt B 163:1–110

Laskar J, Robutel P, Joutel F, Gastineau M, Correia ACM, Levrard B (2004) A long-term numerical solution for the insolation quantities of the earth. Astron Astrophys 428:261–285

Lau KM, Weng H (1995) Climate signal detection using wavelet transform: how to make a time series sing. B Am Meteorol Soc 76(12):2391–2402

Lenz OK (2005) Palynologie und Paläoökologie eines Küstenmoores aus dem Mittleren Eozän Mitteleuropas—Die Wulfersdorfer Flözgruppe aus dem Tagebau Helmstedt, Niedersachsen. Palaeontogr Abt B 271:1–157

Lenz OK, Wilde V, Riegel W, Schaarschmidt F (2005) Klima- und Vegetationsdynamik im Mitteleozän von Messel—eine Neubewertung der palynologischen Daten aus der Kernbohrung 4 von 1980. In: Harms FJ, Schaal S (eds) Current geological and paleontological research in the messel formation. Cour For Senckenbg, vol 255, pp 81–101

Lenz OK, Wilde V, Riegel W (2007a) Recolonization of a Middle Eocene volcanic site: quantitative palynology of the initial phase of the maar lake of Messel (Germany). Rev Palaeobot Palyno 145:217–242

Lenz OK, Wilde V, Riegel W, Heinrichs T (2007b) Distribution and paleoecologic significance of the freshwater dinoflagellate cyst Messelodinium thielepfeifferae gen. et sp. nov. from the Middle Eocene of Lake Messel, Germany. Palynology 31:119–134

Liebig V (2001) Neuaufnahme der Forschungsbohrungen KB 1, 2, 4 und 7 von 1980 aus der Grube Messel (Sprendlinger Horst, Südhessen). Kaupia 11:3–68

Lorenz V (2000) Formation of maar-diatreme-volcanoes. International Maar Conference. Terra Nostra 2000/6:284–291

Lourens LJ, Sluijs A, Kroon D, Zachos JC, Thomas E, Röhl U, Bowles J, Raffi I (2005) Astronomical pacing of late Palaeocene to early Eocene global warming events. Nature 235:1083–1087

Mai DH (1981) Entwicklung und klimatische Differenzierung der Laubwaldflora Mitteleuropas im Tertiär. Flora 171:525–582

Mai DH (1995) Tertiäre Vegetationsgeschichte Europas. Fischer, Jena

Mertz DF, Renne PR (2005) A numerical age for the Messel fossil deposit (UNESCO World Heritage Site) derived from $^{40}Ar/^{39}Ar$ dating on a basaltic rock fragment. In: Harms FJ, Schaal S (eds) Current geological and paleontological research in the messel formation. Cour For Senckenbg 255:67–75

Mertz DF, Renne PR, Wuttke M, Mödden C (2007) A numerically calibrated reference level (MP28) for the terrestrial mammal-based biozonation of the European Upper Oligocene. Int J Earth Sci 96:353–361

Morlet J (1983) Sampling theory and wave propagation. In: Chen CH (ed) NATO ASI Series. Issues in acoustic signal/image processing and recognition I:233–261

Mosbrugger V, Utescher T, Dilcher DL (2005) Cenozoic continental climatic evolution of Central Europe. Proc Natl Acad Sci USA 102:14964–14969

Nickel B (1996) Die mitteleozäne Mikroflora von Eckfeld bei Manderscheid/Eifel. Mainzer Naturwiss Arch Beiheft 18:1–146

Pälike H, Shackleton NJ, Röhl U (2001) Astronomical forcing in late Eocene marine sediments. Earth Planet Sc Lett 193:589–602

Pflug HD (1952) Palynologie und Stratigraphie der eozänen Braunkohlen von Helmstedt. Palaeontol Z 26(1/2):112–137

Pflug HD (1957) Zur Altersfolge und Faziesgliederung mitteleuropäischer (insbesondere hessischer) Braunkohlen. Notizbl Hess Landesamt Bodenforsch Wiesbaden 85:152–178

Pross J, Schmiedl G (2002) Early Oligocene dinoflagellate cysts from the Upper Rhine Graben (SW Germany): paleoenvironmental and paleoclimatic implications. Mar Micropaleontol 45:1–24

Richter G, Clausing A (2004) Süßwasser-Dinoflagellaten aus der Grube Messel. Natur Museum 134(4):129–130

Riegel W, Kaouras G, Velitzelos E (1995) Ecological aspects of coal formation in Neogene basins of Greece. Ann Géol Pays Hellénique 34:649–661

Roehler HW (1993) Eocene climates, depositional environments, and geography, greater Green River Basin, Wyoming, Utah, and Colorado. U.S. Geological Survey Professional Paper, 1506-F

Röhl U, Bralower TJ, Norris RD, Wefer G (2000) New chronology for the late Paleocene thermal maximum and its environmental implications. Geology 28(10):927–930

Röhl U, Norris RD, Ogg JG (2003) Cyclostratigraphy of upper Paleocene and lower Eocene sediments at Blake Nose Site 1051 (western North Atlantic). In:Wing SL, Gingerich PD, Schmitz B, Thomas E (eds) Causes and consequences of globally warm climates in the early Paleogene. Geological Society of America Special Paper 369, Boulder, Colorado, pp 576–589

Röhl U, Brinkhuis H, Strickley CE, Fuller M, Schellenberg SA, Wefer G, Wiliams GL (2004) Sea level and astronomically induced environmental changes in Middle and Late Eocene sediments from the East Tasman Plateau. In: Exon N, Kennett JP, Malone M (eds) The Cenozoic Southern Ocean: Tectonics, Sedimentation and Climate Change Between Australia and Antarctica. AGU Geophys Monog Ser, vol 151, pp 127–152

Röhl U, Westerhold T, Monechi S, Thomas E, Zachos JC, Donner B (2005) The third and final early eocene thermal maximum: characteristics, timing and mechanisms of the "X" event. Geological Society of America, Abstracts with Programs, vol 37(7), p. 264

Rolf C, Pucher R, Schulz R, Wonik T (2005) Magnetische Untersuchungen an Kernen der Forschungsbohrung Messel 2001—Erste Erkenntnisse zum Erwerb magnetischer Remanenzen in Pyroklastika. In: Harms FJ, Schaal S (eds) Current Geological and Paleontological research in the Messel Formation. Cour For Senckenbg, vol 255, pp 47–55

Round FE (1981) The ecology of algae. Cambridge University Press, Cambridge

Round FE, Brook AJ (1959) The phytoplankton of some Irish loughs and an assessment of their trophic status. Proc R Ir Acad 60:168–191

Ruttner F (1952) Planktonstudien der Deutschen Limnologischen Sunda-Expedition. Arch Hydrobiol Suppl 21(1/2):1–274

Schaal S, Schneider U (1995) Chronik der Grube Messel. Kempkes, Gladenbach

Schaarschmidt F (1988) Der Wald, fossile Pflanzen als Zeugen eines warmen Klimas. In: Schaal S, Ziegler W (eds) Messel–Ein Schaufenster in die Geschichte der Erde und des Lebens. Waldemar Kramer, Frankfurt, pp 29–52

Schmitz B, Pujalte V (2007) Abrupt increase in seasonal extreme precipitation at the Paleocene-Eocene boundary. Geology 35(3):215–218

Schöne B, Fiebig J (2009) Seasonality in the North Sea during the Allerød and Late Medieval Climate Optimum using bivalve sclerochronology. Int J Earth Sci 98:83–98

Schuler M (1990) Environnements et paléoclimats Paléogènes. Palynologie et biostratigraphie de l'Eocène et de l'Oligocène inférieur dans les fossés rhénan, rhodanien et de Hesse. Document du BRGM 190:1–503

Schulz M, Mudelsee M (2002) REDFIT: estimating red-noise spectra directly from unevenly spaced paleoclimatic time series. Comput Geosci 28:421–426

Schulz R, Harms FJ, Felder M (2002) Die Forschungsbohrung Messel 2001: Ein Beitrag zur Entschlüsselung der Genese einer Ölschieferlagerstätte. Z Angew Geol 4:9–17

Schwarzbach M (1968) Das Klima des rheinischen Tertiärs. Z Dtsch Geol Ges 118:33–68

Sluijs A, Pross J, Brinkhuis H (2005) From greenhouse to icehouse; organic-walled dinoflagellate cysts as paleoenvironmental indicators in the Paleogene. Earth-Sci Rev 68:281–315

Sluijs A, Schouten S, Donders HD, Schoon PL, Röhl U, Reichart GJ, Sangiorgi F, Kim JH, Sinninghe Damsté JS, Brinkhuis H (2009) Warm and wet conditions in the Arctic region during Eocene Thermal Maximum 2. Nat Geosci 2:777–780. doi:10.1038/NGEO668

Spicer RA, Greer AG (1986) Plant taphonomy in fluvial and lacustrine systems. In: Gastaldo RA (ed) Land plants: notes for a short course. University of Tennessee Department of Geological Sciences, Studies in Geology, vol 15, pp 10–26

Stebich M, Mingram J, Han J, Liu J (2009) Late Pleistocene spread of (cool-)temperate forests in Northeast China and climate changes synchronous with the North Atlantic region. Global Planet Change 65:56–70

Stuchlik E (1994) Neogene pollen flora of Central Europe. Part 1. Acta Palaeobotan Suppl 1:5–56

Tanaka N, Setoguchi H, Murata J (1997) Phylogeny of the family Hydrocharitaceae inferred from rbcL and matK gene sequence data. J Plant Res 110:329–337

Taylor GH, Teichmüller M, Davis A, Diessel CFK, Littke R, Robert P (1998) Organic petrology. Borntraeger, Berlin

ter Braak CJF, Looman CWN (1995) Regression. In: Jongman RHG, ter Braak CJF, Tongeren OFR (eds) Data analysis in community and landscape ecology. Cambridge University Press, Cambridge

Thiele-Pfeiffer H (1980) Die miozäne Mikroflora aus dem Braunkohlentagebau Oder bei Wackersdorf/Oberpfalz. Palaeontogr Abt B 174:95–224

Thiele-Pfeiffer H (1988) Die Mikroflora aus dem mitteleozänen Ölschiefer von Messel bei Darmstadt. Palaeontogr Abt B 211:1–86

Thomson PW, Pflug H (1953) Pollen und Sporen des mitteleuropäischen Tertiärs. Gesamtübersicht über die stratigraphisch und paläontologisch wichtigen Formen. Palaeontogr Abt B 94:1–138

Torrence C, Compo GP (1998) A practical guide to wavelet analysis. B Am Meteorol Soc 79:61–78

Trauth MH, Deino AL, Berner AGN, Strecker MR (2003) East African climate change and orbital forcing during the last 175 kyr BP. Earth Planet Sci Lett 206:297–313

Traverse A (1992) Organic fluvial sediment: palynomorphs and 'palynodebris' in the lower Trinity River, Texas. Ann Mo Bot Gard 79:110–125

Turney CSM, Kershaw AP, Clemens SC, Branch N, Moss PT, Fifiled LK (2004) Millenial and orbital variations of El Niño/Southern Oscillation and high-latitude climate in the last glacial period. Nature 428:306–310

Tyson RV (1995) Sedimentary organic matter. Chapman & Hall, London

Varadi F, Runnegar B, Ghil M (2003) Successive refinements in long-term integrations of planetary orbits. Astrophys J 592:620–630

Wanamaker AD, Kreutz KJ, Schöne BR, Maasch KA, Pershing AJ, Borns HW, Introne DS, Feindel S (2009) A late Holocene paleo-productivity record in the western Gulf of Maine, USA, inferred from growth histories of the long-lived ocean quahog (Artica islandica). Int J Earth Sci 98:19–29

Warnaar J, Bijl PK, Huber M, Sloan L, Brinkhuis H, Röhl U, Sriver R, Visscher H (2009) Orbitally forced climate changes in the Tasman sector during the Middle Eocene. Palaeogeogr Palaeocl 280:361–370

Weber J, Hofmann U (1982) Kernbohrungen in der eozänen Fossillagerstätte Grube Messel bei Darmstadt. Geol Abh Hessen 83:1–58

Westerhold T, Röhl U, Laskar J, Bowles J, Raffi I, Lourens LJ, Zachos JC (2007) On the duration of magnetochrons C24r and C25n and the timing of early Eocene global warming events:

implications from the Ocean Drilling Program Leg 208 Walvis Ridge depth transect. Paleoceanography, 22, PA2201. doi: 10.1029/2006PA001322

Westerhold T, Röhl U, Raffi I, Fornaciari E, Monechi S, Reale V, Bowles J, Evans HF (2008) Astronomical calibration of the Paleocene time. Palaeogeogr Palaeocl 257:377–403

Wetzel RG (1983) Limnology. Saunders College Publications, Philadelphia

Wilde V (1989) Untersuchungen zur Systematik der Blattreste aus dem Mitteleozän der Grube Messel bei Darmstadt (Hessen, Deutschland). Cour Forsch Senckenberg 115:1–123

Wilde V (2004) Aktuelle Übersicht zur Flora aus dem mitteleozänen „Ölschiefer" der Grube Messel bei Darmstadt (Hessen, Deutschland). Cour For Senckenbg 252:109–114

Wilde V, Frankenhäuser F, Lutz H (1993) Algenreste aus den mitteleozänen Sedimenten des Eckfelder Maares bei Manderscheid in der Eifel. Mainzer Naturwiss Arch 31:127–148

Willis KJ, Kleczkowski A, Crowhurst SJ (1999) 124000-year periodicity in terrestrial vegetation change during the late Pliocene epoch. Nature 397:685–688

Wing SL, Harrington GJ, Bowen GJ, Koch PL (2003) Floral change during the initial eocene thermal maximum in the powder river bank, Wyoming. Geol S Am S 369:425–440

Wing SL, Harrington GJ, Smith FA, Bloch JI, Boyer DM, Freeman KH (2005) Transient floral change and rapid global warming at the Paleocene-Eocene boundary. Science 310:993–996

Zachos J, Pagani M, Sloan L, Thomas E, Billups K (2001) Trends, rhythms, and aberrations in global climate 65 Ma to present. Science 292:686–693

Zippi P (1998) Freshwater algae from the Mattagami Formation (Albian), Ontario: Paleoecology, botanical affinities, and systematic taxonomy. Micropaleontology Suppl 1(44):1–78